بسم الله الرحمن الرحيم

PALESTINE POLYTECHNIC UNIVERSITY

COLLEGE OF ENGINEERING AND TECHNOLOGY
DEPARTMENT OF ELECTRICAL AND COMPUTER ENGINEERING

GRADUATION PROJECT REPORT

DESIGN AND CONTROL OF EDDY CURRENT LOADING UNIT

Researched by:

LUAY M. AL-HAFEZ **MOHAMMED M. EHMEDAT**

Supervisor:

Dr. SAMEER H. KHADER

HEBRON – PALESTINE

Feb. 2005

Abstract

Eddy current brake

Eddy current brake unit is used for torque control applications , unlike author torque devices , eddy current brake unit provide absolutely smooth , infinitely controllable torque loads , independent of the speed and operate without any physical contact of interactive members .

As result, with the exception of shaft bearings.

Comparing to the conventional brake system such as hydraulic system which has many disadvantages such as time delay response due to pressure build up, brake bade wear due to contact movement, bulk size, and low braking, the eddy current brake system has no friction element – same smooth torque year by year, high braking, no external electricity to operate is case of permanent magnets, so it is used for accurate tension applications.

The eddy current system that would design has two mean parts: the coil that should be energized with dc current. The second part is the disk connected to the motor shaft.

In this case the brake should be energized from external dc source, and therefore the loading level could be regulated.

Table of contents

Chapter three

Chapter four

Chapter five

Chapter six

Appendix

List of figure

List of tables

Chapter One

- Introduction
- Objectives of the project
- Importance of project
- Literature Review
- Terminology
- Project cost

1.1 Introduction

Eddy current brakes are an abrasion free method for breaking. In high speed trains they offer a good alternative to the mechanical rail brakes which are used nowadays. In such an application the rail represents the part in which the eddy currents are induced. The eddy currents then cause, according to Lentz's rule, the breaking effect.

This project contains five chapters: The first chapter is the introduction of the project it contain the objectives, important of the project, type of braking, some of terminology, Literature Review, time plan and estimated cost.

The second chapter talks about eddy current and eddy current applications such as braking. It discusses how the eddy current produced and the effective of the conductor slot on it. Also talks about the eddy current brake in two modifications, permanent magnet braking and electromagnetic braking.

The third chapter talks about the sensors which measured the output torque and the speed sensor (tachometer).

The fourth chapter contains design of eddy current braking based on electromagnetic method by dc excitation using excited coil. It contains the construction of the eddy current brake and the required analysis.

The fifth chapter describes the control unit and the interfacing between system elements (supply source, loading unit, sensing unit, current regulating unit. DAQ, …).

The sixth chapter talks about the conclusion and some recommendation .

1.2 Objectives of the project

The mains object of this project is to design an eddy current loading unit, applied as mechanical load to a brushless dc motor as partial case.

Also this project has the following educational objectives:

- To observe how eddy current produced in the disc and it's effect on braking level.
- To apply our knowledge in various fields such as power, control, and computer simulation.

1.3 Importance of project

The importance of this project is come from the control of the torque braking has widely range. Also there is no wiring part between drive and driven side.

This means that, there significant losses and the maintenance is easy and rarely .because no friction elements.

1.4 Literature Review

While not discussed much at all in the past, the topic of magnetic braking has dramatically increased in popularity in recent years.

1.5 Terminology

Eddy Current: Localized currents induced in an iron core by alternating magnetic flux. These currents translate into losses (heat) and their minimization is an important factor in lamination design.

Eddy Current Brake: A unit consisting of a rotating member keyed to a straight through, double extension shaft and a field coil assembly. The brake rotor rotates at the speed of the prime mover until the field coil is energized. Rotation of the rotor is slowed by controlling the current in the field coil.

Eddy Current Clutch: A device that permits connection between a motor and a load by electrical (magnetic) means - no physical contact is involved. This method is also used for speed control (by clutch "slippage").

Eddy Current Drive: A unit consisting of a driving member which is the drum assembly, the driven member which is the rotor assembly, and a magnetic member which is the field coil assembly. The driven member is driven by a constant speed AC motor. Control of the eddy current drive is obtained by controlling the current in the field coil.

Electrical Coupling: When two coils are so situated that some of the flux set up by either coil links some of the turns of the other, they are said to be electrically coupled.

1.7 Project cost

Devices	Cost ($)
Personal computer	400
DAQ	350
Electronic device	200
Other requirement	200
Total cost	**1150 $**

Chapter Two

- Eddy currents & Magnetic braking.
- Properties of materials

2.1 Eddy Currents

2.1.1 Introduction

An eddy current is a swirling current set up in a conductor in response to a changing magnetic field. By Lenz's law, the current swirls in such a way as to create a magnetic field opposing the change; to do this in a conductor, electrons swirl in a plane perpendicular to the magnetic field.

The main or working flux in a transformer or machine induces in a winding the useful e.m.f. concerned in energy transfer or conversion. The non-useful leakage flux also produces an e.m.f., which may introduce a loss arising from the disturbance of the current distribution in the conductors of the winding.

The parasitic eddy-currents in an isolated conductor due to its own field are called the skin effect. They arise on account of the inductance of the central parts of the conductor exceeding that of the outer parts. The reactance of the centre is therefore greater, and the current flows consequently more readily in the outer layers of the conductor. But any departure from uniform current density increases the I^2R loss over its D.C. value. The greater induced e.m.f. of self-induction in the middle parts of the conductor causes circulating currents which superimposed on the main current increases the I^2R loss.

In machines and transformers the conductors forming the windings are not, however, isolated, and the effects of alternating leakage fields are intensified by the proximity of ferromagnetic material. There are losses — usually undesirable — in the conductors themselves, and in neighbouring permeable or conducting masses (such as transformer tanks, and the stiffeners and housings of machines) resulting from currents induced therein by the conductors. The boundary shapes differ so radically that it is necessary to deal piecemeal with a variety of combinations of conductors and neighbouring masses.

2.2 Eddy current Brakes

2.2.1 Introduction

A unit consisting of a rotating member keyed to a straight through, double extension shaft and a field coil assembly. The brake rotor rotates at the speed of the prime mover until the field coil is energized. Rotation of the rotor is slowed by controlling the current in the field coil.

Electrically powered eddy current brakes are an abrasion free method for breaking. In high speed trains they offer a good alternative to the mechanical rail brakes which are used nowadays. In such an application the rail represents the part in which the eddy currents are induced. The eddy currents then cause, according to Lentz´s rule, the braking effect.

Sophisticated calculation methods for the determination of the braking and attracting forces of eddy current brakes are important for the design of the brake's magnetic path. It developed that, especially for this problem a 3D-FEM-solver for non-linear materials with movement term. The solver can be incorporated into available software packages. With this solver the design and function of eddy current brakes can be optimized.

Recently, permanent magnet excited eddy current brakes have been developed for subways, trams and local trains. These brakes need a mechanical actuator to turn the magnets in an on and off position. One of the brakes main advantages is safety. In contrast to electrically excited eddy current brakes loop causes a force contrary to that motion.

Mechanical energy being used to move the loop will be turned into electrical energy driving current in the loop. The faster the loop is pulled, the harder the loop will pull back.

Most people can get this far on their own, yet eddy currents still seem strange, though the idea of an eddy current is no different than this.

Just like current being induced in a loop of wire, current 'swirls' or 'eddies' -- little whirlpools of current -- can be induced inside a solid conductive slab. While there is no "wire" inside the slab, the inductance (all conductors are inductors, including capacitors before transients die out; imagine a capacitor acting like a short for high frequencies) of the slab causes nature to move current along the same way it would if there was a circular wire.

So if you moved a slab into a magnetic field or out of a magnetic field, eddy currents would be induced inside the slab that would cause an equal an opposite reaction to the forces being applied to the slab.

Another example to make this clear . . .

The pendulum could swing back and forth, and could attach to a number of different types of conductive rings at the end of it. As it swung, the ring on the end of it would pass between two poles of a very strong very huge magnet (when rolled into a small physics lab, this magnet would discolor all

CRTs in the room) . . .

The first example would be to put a conductive ring (it didn't have to be a ring -- the ring was just how it attached to the pendulum; only the solid part went through the strong part of the magnetic field) at the end of the pendulum and let it swing through. This conductive ring was solid -- like a large dough-nut. The pendulum threw into the field, once the ring came in between the two poles, it stopped immediately. All of its kinetic energy went into moving current inside the conductive ring.

Now, the next example was to take a very similar ring, but this ring had a number of slits cut in it. It was still a ring, but the area that passed between the two poles looked like frayed edges.

This time, the pendulum swung through the poles with no trouble -- it swung back and forth a few times.

The slits cut in the second example had the same effect as breaking the 'loop' in the very first example. If you break the loop, an emf will be generated, but no current will be able to flow. Without any current, no field can be generated.

So by making slits, if there are going to be any eddy currents, they are going to be very small currents that provide very little bleeding off of the kinetic energy.

This type of 'dynamic breaking' can be extended further. Imagine a motor. If you replace the battery of that motor with a light bulb and turn the motor manually, the light bulb may light. If you continue to add more loads than just a light bulb, they might all start to operate, but with more loads, it will become harder and harder to rotate the "backwards motor generator." Removing all of these loads so that there is nothing connecting the two previous battery leads will make the motor rotate easily (assuming low friction/appropriate gear ratio/etc.).

Eddy currents actually do play a part in things like transformers, which is why transformers are usually made of laminated cores that prevent eddy currents.

When a coil of wire surrounds a ferromagnetic core, like iron, for example, of a transformer, the changing magnetic field induces an eddy current in the core, which happens to be conductive as well. If you build the core out of a great deal of layers all separated by an insulator, you can prevent eddy currents. Preventing eddy currents in transformers prevents power loss (currents in resistive materials cause power loss) in the transformer. There are other sources of power loss in a transformer, but those are much more complicated. Even the simplest [moderately large] transformer (not necessarily chokes) will most likely have a laminated core.

2.2.3 Advantage of the eddy current brake

- No contacting or wearing parts
- No friction elements - same smooth torque year after year
- No external electricity to operate
- No magnetic particles to leak or contaminate end products
- Operable in some of the most difficult wet environments
- Brake (with shaft) and clutch (with hollow shaft) available.

2.2.4 Typical Applications:

Generally eddy current clutches are used for take-up applications on slitting and rewinding machinery. But it also builds eddy current designs into all our common hysteresis brake models.

2.3 Magnetic braking:

2.3.1 Introduction

Magnetic braking works because of induced currents and Lenz's law. If you attach a metal plate to the end of a pendulum and let it swing, its speed will greatly decrease when it passes between the poles of a magnet. When the plate enters the magnetic field, an electric field is induced and circulating "eddy currents" are generated. These currents act to oppose the change in flux through the plate, in accordance with Lenz's Law. The currents in turn dissipate some of the plate's energy, thereby reducing its velocity.

[illegible] the eddy currents need a place to produced [illegible] cutting slits in the plate, the damping force [illegible]. When there are enough slits to break up the [illegible] not a large enough area for the currents to form, damping and the plate swings unimpeded through the magnet.

The practical uses for magnetic braking are numerous and commonly found in industry today. This phenomenon can be used to “damp unwanted oscillations in satellites, to eliminate vibrations in spacecrafts, and to separate nonmagnetic metals from solid waste.” Lamination, breaking up a solid piece of metal into thin sheets in order to prevent excessive energy loss due to the eddy currents (similar to our cutting slits in the metal sheet), is also common in motors.

2.3.2 Theory

When the metal plate enters the magnetic field, it experiences a Lorentz force

$$\vec{F} = q\left(\vec{v} \times \vec{B}\right) \quad \text{.............(2.1)}$$

This effects the conduction of electrons in the metal. Here, $\vec{v}$ is the velocity vector of the charge q, and $\vec{B}$ is the magnetic field vector. The force on the electrons induces a current in the metal.

Figure 2.1 shows these “eddy currents” in relation to the metal plate which moves perpendicular to the magnetic

In order to work properly, the eddy currents need a place to produced on it. It can be seen that when cutting slits in the plate, the damping force caused by the magnet decreases. When there are enough slits to break up the metal so that there is not a large enough area for the currents to form, damping does not occur and the plate swings unimpeded through the magnet.

The practical uses for magnetic braking are numerous and commonly found in industry today. This phenomenon can be used to "damp unwanted mutations in satellites, to eliminate vibrations in spacecrafts, and to separate nonmagnetic metals from solid waste." Lamination, breaking up a solid piece of metal into thin sheets in order to prevent excessive energy loss due to the eddy currents (similar to our cutting slits in the metal sheet), is also common in motors.

2.3.2 Theory

When the metal plate enters the magnetic field, it experiences a Lorentz force

$$\vec{F} = q\left(\vec{v} \times \vec{B}\right) \quad \text{...........(2.1)}$$

This effects the conduction of electrons in the metal. Here, $\vec{v}$ is the velocity vector of the charge q, and $\vec{B}$ is the magnetic field vector. The force on the electrons induces a current in the metal.

Figure 2.1 shows these "eddy currents" in relation to the metal plate which moves perpendicular to the magnetic

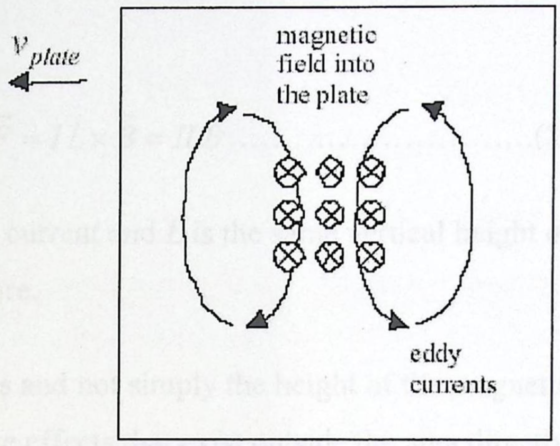

Fig. 2.1 Induced currents in the metal plate.

Faraday's law,

$$e = \frac{d\Phi}{dt} = \frac{d}{dt}\int \vec{B} \circ d\vec{A} \quad \text{...........} \ (2.2)$$

To equate this electromotive force to the velocity of the plate. This involves converting the differential area to a known height times a differential width (*dA* = *L dx*), and relating the differential width to a differential time using velocity. This cances out the integral, allowing use to write the electromotive force as

$$e = BL\upsilon \quad \text{....................} (3.2)$$

Besides inducing the eddy currents in the metal plate, the magnet exerts a force on the currents inside its field. This is the retarding force associated with the braking:

$$\vec{F} = I\vec{L} \times \vec{B} = ILB \ldots\ldots\ldots\ldots\ldots\ldots\ldots\ldots\ldots(2.4)$$

Where I is the current and L is the same vertical height of the effective magnetic field as before.

The reason this and not simply the height of the magnetic poles is used is because of the fringe effects that exist outside the area directly between the two poles of the magnet. This length is determined to be the full width at half height of the Gaussian magnetic field. The simplification in (4) can be made because the length L is perpendicular to the magnetic field.

The calculates of the resistance the currents encounter inside the metal using the conductivity (σ) of the metal and the same area simplification as before:

$$R = \frac{L_R}{\sigma A} = \frac{L_R}{\sigma c x} \ldots\ldots\ldots\ldots\ldots\ldots (2.5)$$

Where L_R is the effective length over which the currents will form and c is the thickness of the metal plate. Ohm's law lets us write a current in terms of the voltage and resistance associated with it. Using equation (2.3) And (2.5), the magnitude of the eddy currents can be written as

$$I = \frac{e}{R} = \frac{\sigma.c.x.B.L}{L_R} v \ldots\ldots\ldots(2.6)$$

This allows us to rewrite the force in Eq. (2.4) in terms of an unknown (LR), measurable constants, and a varying parameter (velocity):

$$F = \frac{\sigma.c.x.B^2.L^2}{L_R} v \text{ ....(2.7)}$$

However, the magnetic field strength B varies with x. To eliminate this dependence, Gadwell performs a simple rectangular approximation of the sum over all positions. The result is the equation we will plot and use to calculate the effective length LR;

$$F = m.a = \frac{\sigma.c.L^{\backslash}.B_{eff}^2.L^2}{L_R} v \text{ ....(2.8)}$$

Where

$$L^{\backslash} = \sum_i^n \Delta x_i \text{ ....(2.9)}$$

And

$$B_{eff} = \frac{B_{max}}{2} \text{ ....(2.10)}$$

2.3.3 Experimental of magnetic brake

Magnetic braking was accomplished by running copper plate between the pole of large magnetic, This plate have several run where done by pushing the plate with different initial velocity. Fig. 2.2

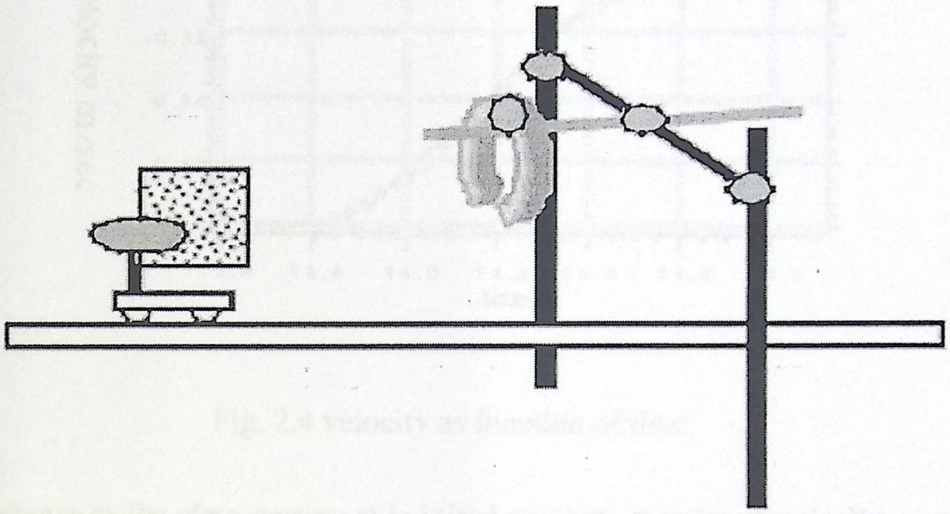

Fig. 2.2 Experimental of magnetic brake.

In order to test the behavior of magnetic braking the same running plate was performed while varying the number of slot in the metal plate. Fig 2.3

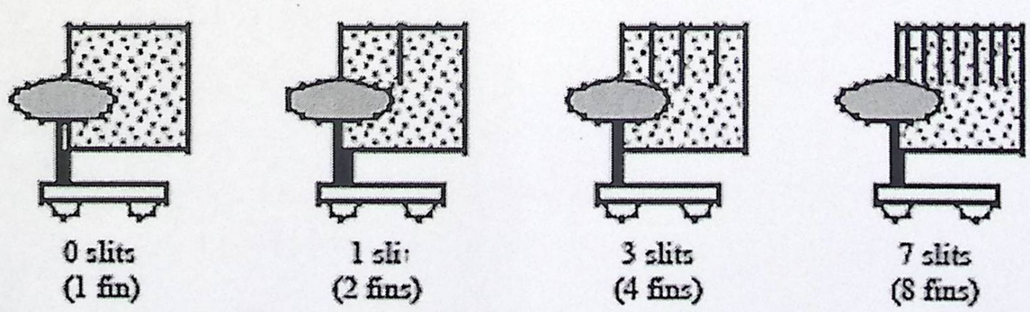

Fig 2.3 cutting slits in the metal sheet

2.3.4 Results

The result (see fig 2.4) show velocity data as function of time .

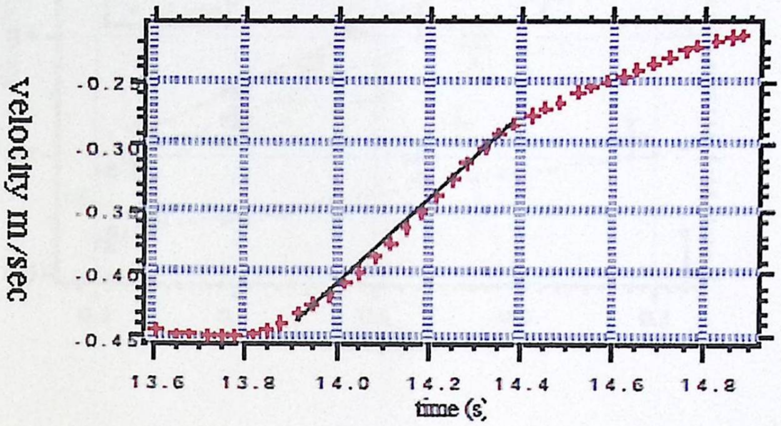

Fig. 2.4 velocity as function of time

It shows as the plate starting at in initial velocity, then the drastically slowing while under the magnet. Afterwards, it slows with a different acceleration, due to friction and air resistance.

The result (see Fig2.5) shows a plot of the force and velocity data for various slits.

experienced by it. Then, our observations reveal that the force on a particular substance is proportional to the mass of

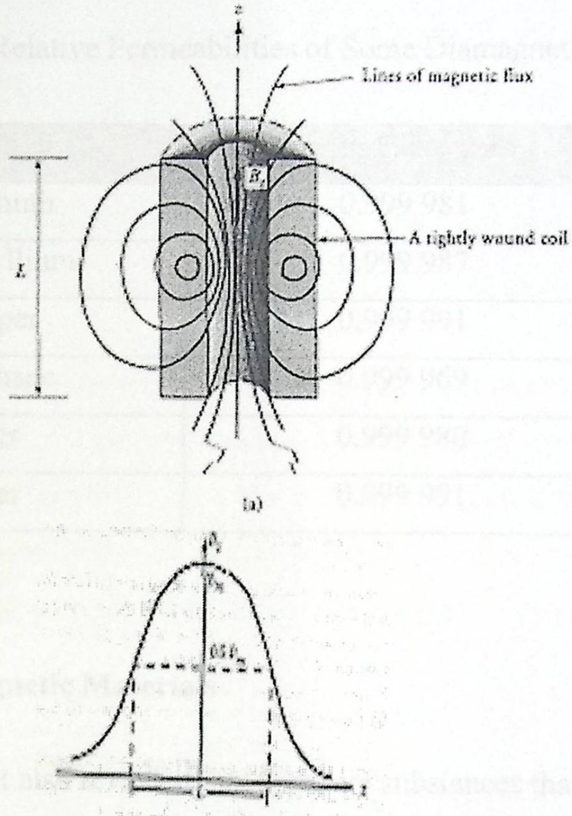

Figure 2.6 (a) A solenoid, (b) Graph of the magnetic flux density along the axis of the solenoid.

The sample and is independent of its shape as long as the sample size is not too large. We also observe that some samples are attracted toward the region of stronger field and other samples are repelled.

2.4.1 Diamagnetic Materials

Those substances that experience a feeble force of repulsion are called diamagnetic. From our experiment we found that bismuth, silver, and copper are diamagnetic materials.

The permeability of a diamagnetic material is slightly less than the permeability of free space. The permeabilities of some diamagnetic materials are given in Table 2.1.

Table 2.1: Relative Permeabilities of Some Diamagnetic Materials

Material	Relative Permeability
Bismuth	0.999 981
Beryllium	0.999 987
Copper	0.999 991
Methane	0.999 969
Silver	0.999 980
Water	0.999 991

2.4.2 Paramagnetic Materials

Our experiment also revealed that there are substances that experienced a force of attraction. Substances that are pulled toward the center of the solenoid with a feeble force are called paramagnetic. These substances exhibit slightly greater permeabilities than that of free space. A list of some paramagnetic materials and their relative permeabilities is given in Table 2.2.

Table 2.2: Relative Permeabilities of Some Paramagnetic Materials

Material	Relative Permeability
Air	1.000 304
Aluminum	1.000 023
Oxygen	1.001 330
Manganese	1.000 124
Palladium	1.000 800
Platinum	1.000 014

Since the force experienced by a paramagnetic or a diamagnetic substance is quite feeble, for all practical purposes we can group them together and refer to them as nonmagnetic materials. It is a common practice to assume that the permeability of all nonmagnetic materials is the same as that of free space. These materials are of no practical use in the construction of magnetic circuits.

2.4.3 Ferromagnetic Materials

Substances like iron were literally sucked in by the magnetic force of attraction in our above-mentioned experiment. These substances are called ferromagnetic. The magnetic force of attraction experienced by a ferromagnetic material may be 5000 times that experienced by a paramagnetic material.

To describe fully the magnetic properties of materials, we need the concept of quantum mechanics, which is considered to be beyond the scope of this book. However, we can use the theory of magnetic domains containing magnetic dipoles to explain ferromagnetism.

Chapter three

- Sensors

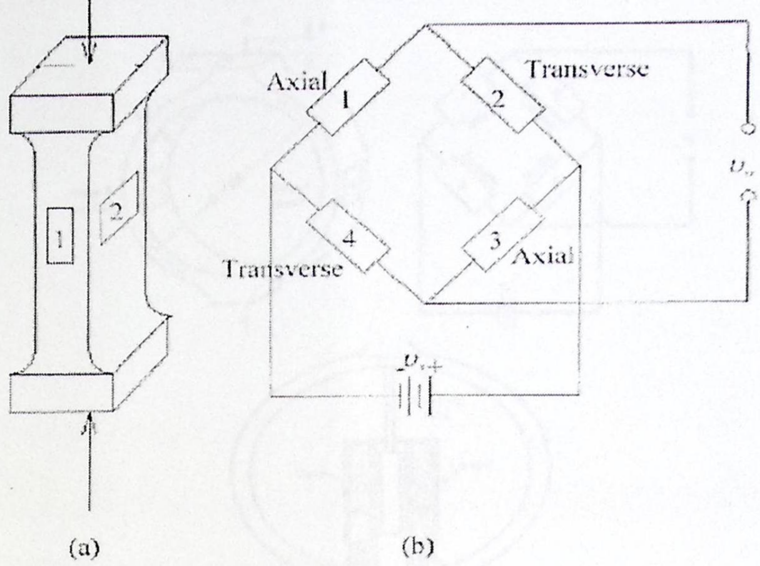

Fig (3.1) link type load cell

3.1.2 Beam-Type Load Cell

This type is commonly used for measuring low-level loads. It consists of a simple cantilever beam with two strain gages on the top of surface and two strain gages on the bottom surface as shown in figure (3.2a) . The gages are connected into a Wheatstone bridge as shown in figure (3.2b).

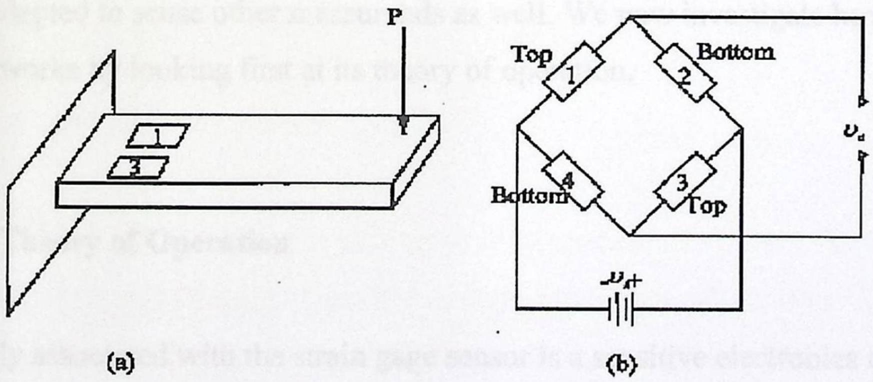

Fig (3.2) beam type load cell

3.1.3 Ring-Type Load Cell

This type incorporates a proving ring as the elastic element. The ring element can be designed to cover a very wide range of loads by varying the radius R, the thickness t, or the depth w of the ring.

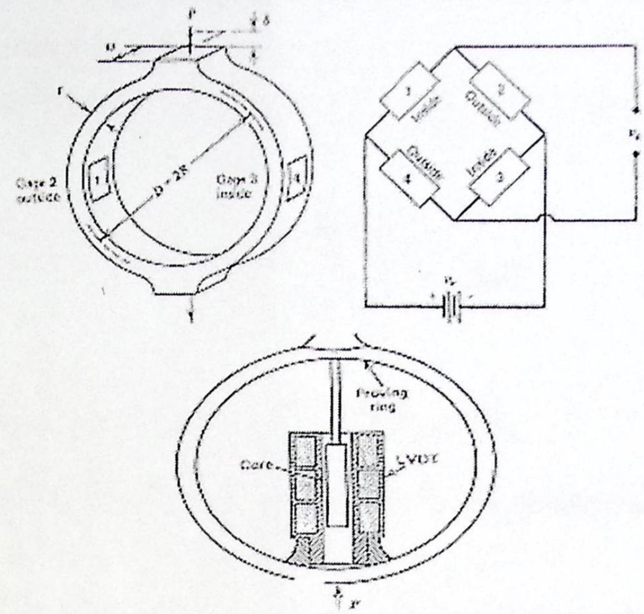

Fig (3.3) ring type load cell

3.2 Strain gage

The strain gage is a resistive device, whose operation is very closely tied to equation (3.1)

$$R = \rho \frac{1}{A} \quad (3.1)$$

The strain gage is used for the detection of stress and strain, although it can readily be adapted to sense other measurands as well. We now investigate how the strain gage works by looking first at its theory of operation.

3.2.1 Theory of Operation

Closely associated with the strain gage sensor is a sensitive electronics circuit used for detecting very small electrical resistance changes. These changes occur in the wire like conductors that comprise the gage's main construction feature. The resistance changes are produced by the stretching of these wires, caused, in turn, by a force applied to the gage's body. In another form of strain gage construction the wire is replaced by a solid-state semi conducting material whose internal electrical resistance changes with the stress applied. The sensing of stress or strain using this method takes advantage of the phenomenon called piezoresistivity. However, we must first define the terms stress and strain.

Stress is defined as follows:

$$stress = \frac{force}{area} \qquad (3.2)$$

Where:

Stress = units of pressure (i.e., N/m^2, lb/in^2, etc.)

Force = force applied either in tension or in compression on an object perpendicular to a surface on that object (N, Ib)

Area = area of an object that is perpendicular to the force applied (m^2, ft^2)

Strain is defined as follows:

$$strain = \frac{\text{change in length of object due to stress applied}}{\text{original length of object}} \qquad \ldots(3.3)$$

Where

Strain is measured in the units m/m, in./in., and the like.

Figure (3.4) illustrates how the piezoresistivity process takes place. A force, F is applied to both ends of loops of conducting material such as metallic wires. As this happens, the conductors become stretched, causing their overall length to increase. This, in turn, causes the conductor's cross-sectional area to decrease, which causes an increase in the conductor's total resistance according to eq. (3.1). The particular gage illustrated in Figure (3.4) is called an unbonded strain gage.

3.2.2 Wheatstone bridge

The change in electrical resistance described above is quite small, as pointed out earlier. As a result, a circuit especially designed to detect very small resistance changes must be used along with the strain gage to detect the gage's very weak

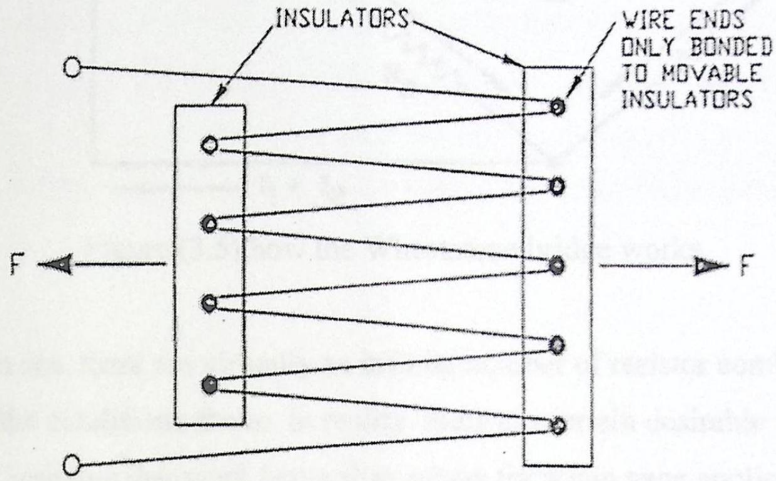

Figure (3.4) typical unbounded strain gage construction.

Responses to stress. This circuit, shown in simplified form in Figure (3.5), is called a Wheatstone bridge. The circuit works like this:

Four resistors are wired in the manner shown, with a galvanometer as a very sensitive: current detector. A voltage source, E, produces two opposing current flows in the legs of the resistance bridge as shown. If the resistance values are adjusted properly so that I_1 equals I_2, it is possible to cause a net current of zero to occur through the galvanometer. This happens only if the following resistor ratios are maintained:

$$\frac{R_1}{R_2} = \frac{R_3}{R_4}$$

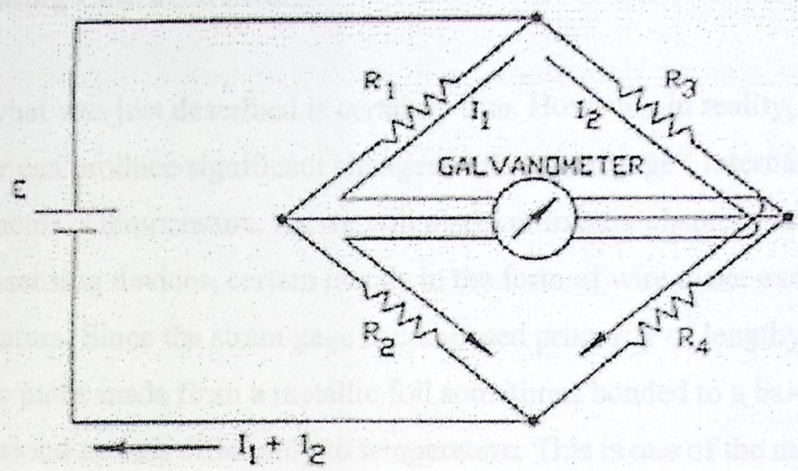

Figure (3.5) how the Wheatstone bridge works.

As you can see, there are virtually an infinite number of resistor combinations that will satisfy the conditions above. In reality, there are certain desirable combinations of resistors that work better than others for strain gage applications, but that is beyond the scope of our discussion.

If one of the resistors in eq.(3.4)

$$A = \frac{\pi d^2}{4} \quad ....(3.4)$$

is made variable, say R_1, and one of the other resistors, say R_4, is replaced by the dc resistance of our strain gage. it is possible to adjust R_1 so that the ratio formed by R_3/R_4 is precisely equal to the ratio formed by the fraction R_1/R_2 . When this occurs, there will be no current flow through the galvanometer; the galvanometer's indicator needle will read zero in a straight upward position. A mismatch of these two ratios will produce an imbalance of currents in each of the two current paths of the bridge, causing the galvanometer's needle to deflect to one side or the other of center zero. Once the balanced or nulled condition has been reached, any movement of the galvanometer's needle to the right or left of center zero will be a certain indication of a change in the strain gage's resistance brought on by a stressed condition to the gage.

3.2.3 Operating Characteristics

In theory, what was just described is certainly true. However, in reality, another more subtle factor can produce significant changes in the strain gage's internal resistance. That factor is temperature. As we will discover in later chapters dealing with temperature-sensing devices, certain metals in the form of wire make excellent temperature indicators. Since the strain gage is composed primarily of lengthy wire strands or metallic paths made from a metallic foil sometimes bonded to a base or substrate, they respond no less differently to temperature. This is one of the more notable and undesirable characteristics of a strain gage.

So how can we nullify the effects of temperature? The technique is surprisingly simple. Figure (3.6) illustrates how it is done. Using the example above, where R_1 was the variable balancing resistor for the Wheatstone bridge and R_4 was the strain

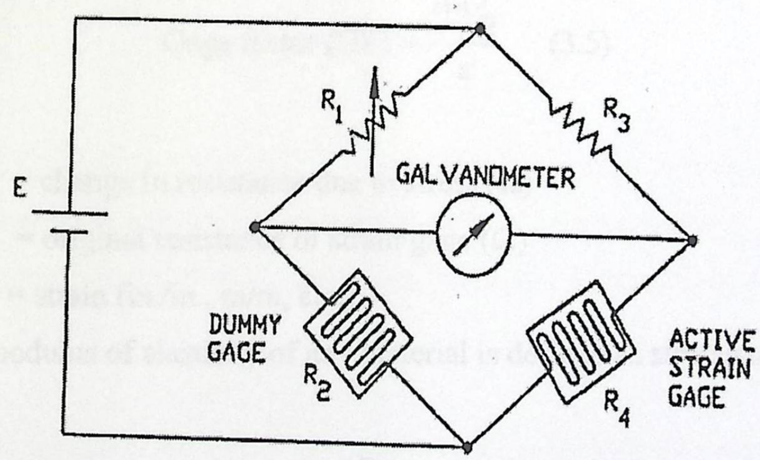

Figure (3.6) nullifying the effects of temperature in a strain gage circuit.

gage, we could insert a duplicate gage into the bridge circuit that was not subject to the measured strain. This duplicate gage would be subjected to the same temperature as that experienced by the stressed gage. The duplicate gage, or dummy gage as it is often called, can be inserted in place of R_2 to offset the temperature-created resistance in the stressed strain gage, R_3

Another circuit scheme is shown in Figure (3.7). Here we see all four of the Wheatstone bridge resistors replaced with strain gages. Balancing resistors R_{b1} and R_{b2} are applied in series with two adjacent arms for equalizing purposes, one compensating for thermal drift, the other for bridge balancing. Any temperature variations external to the bridge will cause all four gages to respond equally (assuming that all four gages are equally matched), causing any temperature-induced resistance variations lo be canceled.

Another notable characteristic of the strain gage has to do with its output signal when subjected to stress. Associated with each strain gage is its gage factor. The gage factor for any strain gage compares that gage's output, expressed as a ratio of resistance change to the gage's original resistance, to its input, expressed as a strain.

In other words, this comparison is the gage's sensitivity. In this particular case, the figure calculated has no units:

$$\text{Gage factor (GF)} = \frac{\Delta R / R}{\varepsilon} \qquad (3.5)$$

Where:

ΔR = change in resistance due to stress (Ω)

R = original resistance of strain gage (Ω)

∈ = strain (in./in., m/m, etc.)

Since the modulus of elasticity of any material is defined as stress/strain, we can say that

$$\varepsilon = \frac{P}{E} \quad \ldots\ldots(3.6)$$

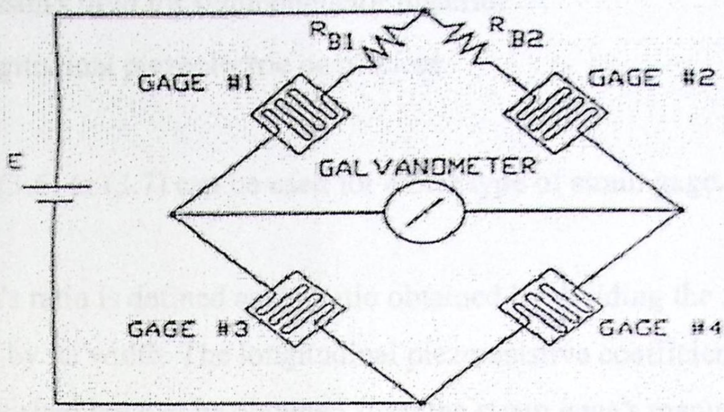

Figure (3.7) another method for reducing temperature effects in a Wheatstone bridge, strain gage circuit‹

Where :

Є = resultant strain (in./in., m/m).

p = applied stress (Ib/in², N/m²).

E =modulus of elasticity of the gage's wire (Ib/in², N/m²).

Equation (3.7) may now be rewritten as

$$GF = \frac{\left(\Delta R/_R\right)E}{P} \qquad (3.7)$$

As can be seen from eq.(3.6) or (3.7), the higher the change in resistance for a given applied stress to the gage, the higher the gage factor. Or conversely, the higher the gage factor figure associated with each gage, the higher its sensitivity to the stress applied.

The gage factor equations above are usually associated with wire strain gages. strain gages are also constructed from certain semiconductor materials having internal strain-resistance behavior similar to that of wire. Often, for these materials the gage factor is defined somewhat differently:

$$GF = 1 + 2\mu + \gamma E \qquad (3.8)$$

Where:

GF = gage factor

μ= Poisson's ratio for semiconductor material

γ = longitudinal piezoelectric coefficient

However, eq.(3.6) or (3.7) can be used for either type of strain gage.

Note: Poisson's ratio is defined as the ratio obtained by dividing the stressed length of a material by its width. The longitudinal piezoresistive coefficient is a figure not often found published but can be obtained from the strain gage's manufacturer.

Semiconductor gages display some interesting characteristics compared to metal gages. Gage factors for semiconductor gages tend to run much higher, often by factors of 20 or greater. These gages are usually smaller, due to their higher gage factors, and they display a much wider resistance range for a given applied stress.

This, of course, accounts for the higher gage factors. Semiconductor gages tend to have less hysteresis than do metal gages. Also, semiconductor gages lend to be more rugged than their metal counterparty. Unfortunately, the semiconductor strain gage suffers from the same temperature-sensitivity problem as docs the wire strain gage.

Typical gage factors for wire and foil strain gages range between 2 and 5. Gages made from semiconductor material typically range from around 40 to as high as 180. All strain gages have a most sensitive response direction or axis relative to the applied stress. This is illustrated in Figure (3.8). Notice that the most sensitive axis is parallel to the lengths of conductors in the grid.

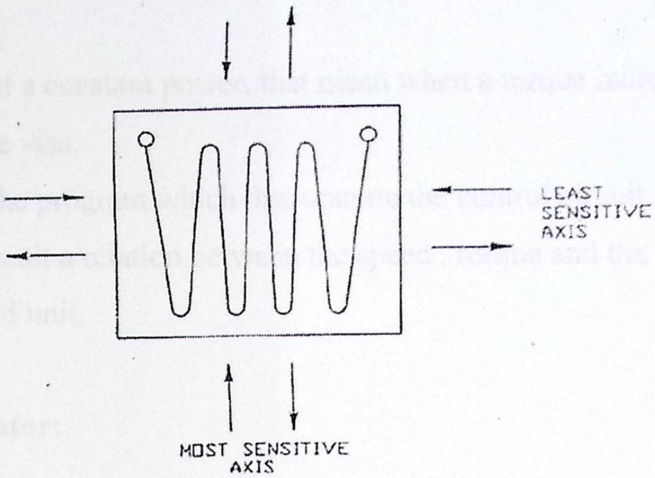

Figure (3.8) Strain gage showing sensitivity axes

3.2.4 Typical Construction

As already mentioned, strain gages are manufactured from either wire or foil strain detectors, or from semiconductor materials (primarily silicon, and germanium). As for all other sensing transducers, strain gages come in a variety of sizes and shapes.

Looking first at their construction, there are two major types, bonded and unbonded construction. In bonded construction the strain-sensing material forming the grid is bonded or fixed rigidly to a base called the substrate or backing.

The backing is constructed of a moisture- and shock-resistant material usually made from an epoxy or plastic material. The strain grid itself is bonded to the backing by means of an epoxy, or the grid may be chemically etched onto the substrate. When the bonded gage is subjected to a stress, the stress is applied to the entire bonded structure.

In an unbonded strain gage. the grid is allowed to have independent motion relative to its backing so that the applied stress is applied only to the grid and not to the backing, as in the case of the bonded gage.

So we choose a tachometer which measured a speed after loading , an this speed as a feedback for control circuit .

When we work at a constant power. that mean when a torque increase the speed will decrease. And vice visa.

When we write the program which that operate the control circuit we make a table which contain circuit a relation between the speed , torque and the value current which energize the field unit.

3.3 Tachogenerator:

An electromechanical generator is a device capable of producing electrical power from mechanical energy. When not connected to a load resistance, generators will generate voltage roughly proportional to shaft speed. With precise construction and design, generators can be built to produce very precise voltages for certain ranges of shaft speeds, thus making them well-suited as measurement devices for shaft speed in mechanical equipment.

A generator specially designed and constructed for this use is called a tachometer or tachogenerator as shown in figure (3.9).

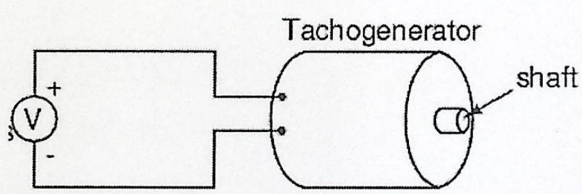

Figure (3.9): Tachogenerator diagram

Chapter four

- Design of eddy current loading unit

Design of the eddy current load unit

4.1 Introduction

Eddy current brake are used as torque motor control , specially in critical torque application , in this chapter the design , construction , working principle and analysis of eddy current braking will discuss .

4.2 Eddy Current Brake

Definition: A unit consisting of a rotating member keyed to a straight through, double extension shaft and a field coil assembly. The brake rotor rotates at the speed of the prime mover until the field coil is energized. Rotation of the rotor is slowed by controlling the current in the field coil.

4. 3 Type of the eddy current brake:

There is two type of the eddy current brake:

- Permanent magnetic brake.
- Electromagnetic brake.

4.3.1 Permanent magnetic brake.

4. 3.1.1 Construction:

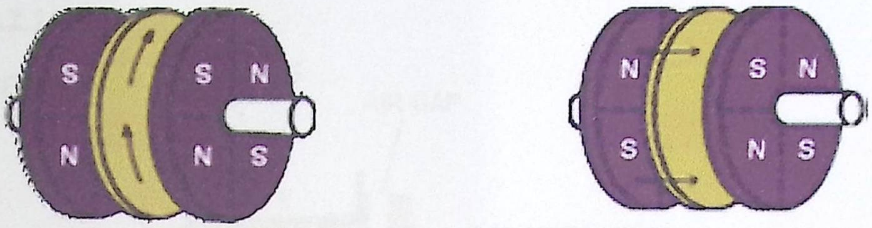

Fig (4.1) permanent magnet brake

This construction consist two parts:

- Permanent magnetic.
- Rotating disc mounted on the motor shaft.

4. 3.1.2 The principle of operation

There are two cases:

4. 3.1.2.1 First case

When like poles face each other, they produce maximum magnetic saturation of the hysteresis disc, forcing lines of flux to travel circumferentially through the hysteresis disc. This produces maximum torque.

4.3.1.2.2 Second case

When opposite poles face each other, they produce minimum saturation of the hysterics disc. The lines of flux travel right through the hysterics disc.

Combinations of adjustment angles between these two extremes give infinite adjust ability. Because there are no contacting surfaces, the setting can be maintained indefinitely.

4.3.2 Electromagnetic brake

4.3.2.1 Construction

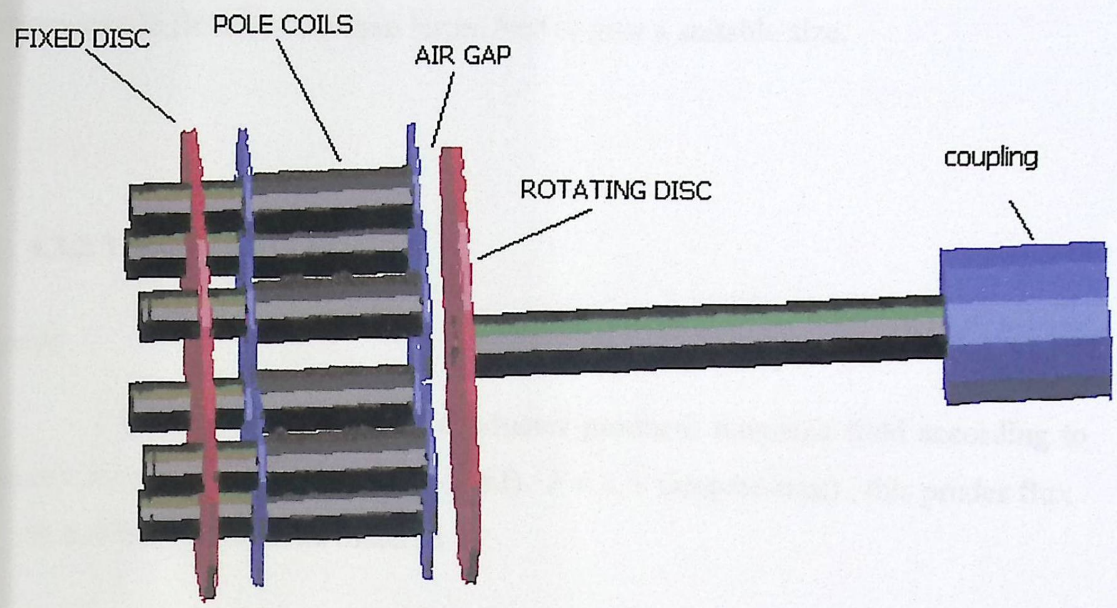

Fig (4.2) construction of the brake system

.

This unit consists:

1- Excitation coil which energized by dc current.(pole coils)

2- Ferromagnetic material,

3- Rotating disc on the motor shaft. .

4. 3.2.2 The Principle of operation

The working principle is based on the creation of eddy currents within a metal disc rotating on the shaft of the motor , which set up a force opposing the rotation of the disc. If the electromagnet is not energized, the rotation of the disc is free and accelerates with the shift of motor. When the electromagnet is energized, the force is effect on the disc the current exciting the electromagnet is varied by a some way, the braking torque varies in direct proportion to the value of the current.

We chose this design because it easy to control flux by change the DC current which energize the coil. And easy to make on or off this current.

We choose the number of pole is six to make the distance which effect by the electromagnetic field is more than large. And to give a suitable size.

4.3.2.3 Analysis of braking

Theory:

Every current carrying conductor produces magnetic field according to amperes law (magnetic motive force –mmf). $F = I.N$ (ampere-turn) , this prudes flux So the flux in magnetic material is :

$$\phi = \frac{F}{R} \quad \text{(Wb).....(4.1)}$$

R :the reluctance of material (ampere-turn per Weber)

$$R = \frac{L}{\mu A} \quad \text{...(4.2)}$$

Where:

L : the mean length of magnetic path

μ : permeability of magnetic material (H/m)

$$\mu = \mu_r \mu_0$$

μ_r : The relative permeability of material

μ_0 : The permeability of space $4\pi \times 10^{7}$

A : cross section area of material

So, The magnetic flux density in magnetic material is :

$$B = \phi / A \quad ...(4.3)$$

Now , for disc rotate in magnetic field , voltage (E) Will be induced across the disc (according to faradays law),

$$E = BL\upsilon \quad ...(4.4)$$

Where:

E: is the induced voltage. (V)

L: is the effective length of the electromagnetic pole.(m)

v: is the speed. (m/sec)

B: flux density (T)

The direction of induced voltage can know by Right –hand- rule.

Thus, the induced voltage that appear on disc will generate current on the disc , so force will act on the disc . (Law of electrodynamics force effect)

** In a current carrying conductor placed in magnetic field ,the force that act upon it equal BIL and has direction can be known by left-hand-rule .

** but for a current carrying disc placed in magnetic field , the force that act upon it is very difficult drive it expression , a person who's name J.H.Wonterses drive it expression . which is:

$$Fe = \frac{1}{4}\frac{\pi}{\rho}D^2 d.B^2 cv \quad ....(4.5)$$

Where:

Fe: braking force,

ρ: specific resistance of disc material ($\Omega.m$)

D: diameter of soft iron pole,(m)

d: disc thickness,(m)

V: tangential speed,(m/s)

B: flux density (T)

C: proportionality factor,

$$c=\frac{1}{2}\left[1-\frac{1}{4}.\frac{1}{\left(1+\frac{r_1}{A}\right)^2\left(\frac{A-r_1}{D}\right)^2}\right] \quad \ldots(4.6)$$

Where:

r1: the distance between the canter of disc and the canter of pole.

A: cross section area of the disc.

Thus, the braking torque on the disc is :

$$T = F_e \times r \quad \ldots.(4.7)$$

Where, r radius of disc.

***** **design calculations:**

** calculated the braking force & torque, eddy current, reluctance, and turn number of coil.

→ Calculated braking force and torque

let we have the following value :

$$B_{\max}=0.7T$$

$D=1.6$ cm (diameter of pole with coil)

$$R=\frac{D}{2}=0.8cm$$

. Resistivity of aluminum disc $\rho_{AL} = 2.82 \times 10^{-8}(\Omega.m)$

. Resistivity of copper disc $\rho_{CU} = 7 \times 10^{-8} (\Omega.m)$

σ = conductivity = $1/\rho$

$d = 2mm$ Thickness of the disc.

$$\omega = \frac{2\pi.n}{60}$$ Where n = 500 rpm.

$$v = \omega r = \frac{2\pi * 500}{60} = *0.075 = 3.925$$

We have two cases:

1- If we have aluminum disc.

2- If we have copper disc.

1- Using aluminum disc.

From equation (4.6)

$$c = \frac{1}{2}\left[1 - \frac{1}{4}.\frac{1}{\left(1+\frac{r_1}{A}\right)^2\left(\frac{A-r_1}{D}\right)^2}\right]$$

$$Fe = \frac{1}{4}\frac{\pi}{\rho}D^2 d.B^2 cv$$

r1 = 0.05 m

$$A = \frac{\pi D^2}{4} = \pi * \left(\frac{1.6 * 10^{-2}}{4}\right)^2 = 2.0096 * 10^{-4}$$

$$=\frac{1}{2}\left[1-\frac{1}{4}\left(\frac{1}{\left(1+\frac{0.05}{2.0096\times10^{-4}}\right)^{2}\left(\frac{2.0096\times10^{-4}-0.05}{1.6*10^{-2}}\right)^{2}}\right)\right]=0.449$$

From equation (4.5)

Braking force on aluminum disc

$$Fe=\frac{1}{4}\frac{\pi}{\rho}D^{2}d.B^{2}cv$$

$$Fe=\frac{1}{4}.\frac{\pi}{2.82*10^{-8}}\left(1.6*10^{-2}\right)^{2}0.002*0.7^{2}*0.499*3.925$$

$F_{e\,AL}=13.678N$ (Braking force per pole)

$F_{eALT}=13.678\times3=41.034N$ (Braking force per three pair of pole)

$$T_{brakingAL}=F_{eALT}\times r=41.034\times0.075=3.077N.m$$

$F_{eCU}=22.689\,N$ Braking force on copper disc per one pole

$F_{eCUT}=22.689\times3=68.67N.m$ (braking force per three pair of pole)

$$T_{brakingAL} = F_{eALT} \times r = 68.67 \times 0.075 = 5.1 N.m$$

Calculated eddy current on the disc:

1- for aluminum disc:

$$F_{Braking} = I_{eddy} LB$$

Where, L = 0.05 , the distance between the center of two poles

$$I_{eddy} = \frac{F_{eALT}}{LB} = \frac{41.034}{0.05*0.7} = 1172.4 A$$

2- for copper disc:

$$I_{eddy} = \frac{F_{eCUT}}{LB} = \frac{68.067}{0.05*0.75} = 1944.77 A$$

Séance the eddy current on copper disc is height than the eddy current on aluminum disc ,so losses on copper disc is large compare with aluminum disc , so we chose aluminum disc on us design .

Calculation for the reluctance →

The equivalent circuit of reluctance is:

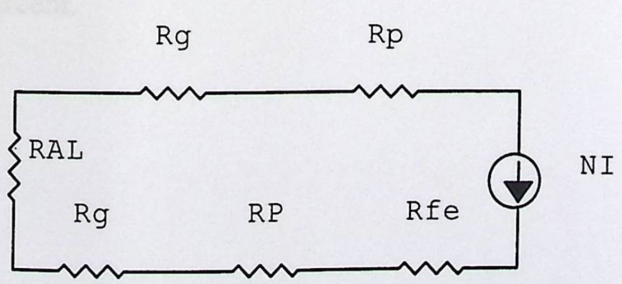

$$R_T = 2R_g + 2R_p + R_{fe} + R_{AL}$$

Where:

Rg : air gap reluctance .

Rp : pole reluctance .

RAl : aluminum disc reluctance .

RFe : iron disc reluctance .

RT : total reluctance of equivocate circuit.

** Air gap reluctance:

$$R_g = \frac{g}{\mu_\circ . A_g}$$

Where:

g = 0.002 m (gap distance)

Ag: cross section area of gap

$$A_g = A_p = \frac{\pi D^2}{4} = \pi * \left(\frac{1.6 * 10^{-2}}{4}\right)^2 = 2.0096 * 10^{-4} m^2$$

$$R_g = \frac{0.002}{4\pi * 10^{-7}(2.0096 * 10^{-4}) * 1.05} = 7546428.04 \text{ amper.turn per Weber}$$

The value 1.05, séance the effect of fringing increase the air gab cross section by 5 percent.

The path of flux passes from one pole to aluminum disc than to the second pole so , there is two gap .

$R_{gT} = 2R_g = 115092856.08$ amper.turn per Weber

** Pole reluctance :

$$R_p = \frac{L}{\mu_r . \mu_\circ . A_P}$$

L : length of pole

$$A_P : 4.0096 \times 10^{-4} m^2$$

$\mu_r = 4000$ (Relative permipility of iron)

$$R_P = \frac{0.07}{4000 * 4\pi * 10^{-7} * 2.0096 * 10^{-4}} = 692332.807 \text{ amper.turn per Weber}$$

Since the flux passes through two poles , so

$R_{pT} = 2 \times R_P = 138665.61$ amper.turn per Weber

→ Aluminum disc reluctance

$$R_{AL} = \frac{L}{\mu_r . \mu_\circ . A_{AL}}$$

L= 0.05 m (distance between two poles)

$$\mu_{rAL} = 1$$

$$A_{AL} = d \times D = 0.002 \times 0.016 = 3.6 \times 10^{-5} m^2$$

$$R_{AL} = \frac{0.05}{1*4\pi*10^{-7}*(3.6*10^{-5})} = 1105803255 \text{ amper.turn per Weber}$$

iron disc reluctance :

$$R_{Fe} = \frac{L}{\mu_r.\mu_\circ.A}$$

$$= \frac{0.05}{4000*4\pi*10^{-7}*3.6*10^{-5}} = 276450.81 \text{ amper.turn per Weber}$$

$$\mapsto \quad R_T = 1121311228 \quad \text{amper.turn per Weber}$$

** Calculation turns number of coils :(using aluminum disc)

Φ=BA=

$$= F_{braki}/R_T = NI_{DC}/R_T$$

$$NI_{DC} = R_T BA$$

$$F_{brak} = I_{eddy} LB$$

$$B = F_{brak}/I_{eddy}L$$

$$NI_{DC} = \frac{R_T A F_{brake}}{I_{eddy} L} = \frac{1121311228 \times 2.0096 \times 10^{-4} \times 41.034}{1172.4 \times 0.05}$$

Ampere- turn $NI_{DC} = 786.854$

I_{DC} : DC current that energized the coil

= 5 ampere

So:

N = 1577.37 turn per pole

N/6 = 262 per pole

** Calculation cross section area of the wire that will be used in coils:

Let:

$$I = 5A$$

$$J = (\ 2.5 - 4.5\ ) A/mm^2$$

$$A = \frac{I}{J} = \frac{4}{5} = 1.25mm^2$$

Let J = 4 A/mm2

$$d = \sqrt{\frac{A}{0.785}}$$

$$= \sqrt{\frac{1.25}{0785}}$$

$$d = 1.26mm$$

3.3.3 Factors affecting eddy current response

The main factors are:

- **Material conductivity**

The conductivity of a material has a very direct effect on the eddy current flow: the greater the conductivity of a material the greater the flow of eddy currents on the surface. Conductivity if often measured by an eddy current technique, and inferences can then be drawn about the different factors affecting conductivity, such as material composition, heat treatment, work hardening etc.

- **Permeability**

This may be described as the ease with which a material can be magnetized. For non-ferrous metals such as copper, brass, aluminum etc., and for austenitic stainless steels the permeability is the same as that of 'free space', i.e. the relative permeability (μ_r) is one. For ferrous metals however the value of μ_r may be several hundred, and this has a very significant influence on the eddy current response, in addition it is not uncommon for the permeability to vary greatly within a metal part due to localized stresses, heating effects etc.

- **Geometry**

Geometrical features such as curvature, edges, grooves etc. will exist and will effect the eddy current response.

Chapter five

- Control system

CONTROL SYSTEM

We can show this chapter by the following block diagram in figure (5.1). And we well discuss all blocks later.

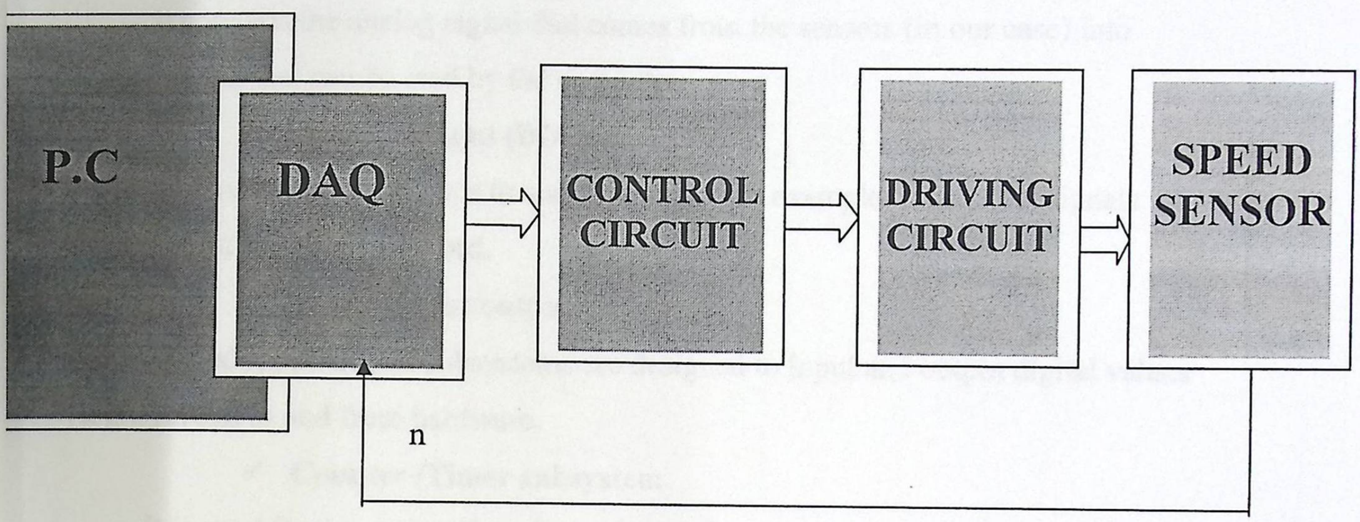

Fig. (5.1) general blockdiagram

5.1 P.C.

we use the personal computer to control this system by writing the program in C-language and send the value to loaded the motor (system).

And the program can see in appendix.

5.2 DAQ (interfacing unit)

We use the DAQ (Data Acquisition Card) as an interfacing unit and to convert the values (signals) from digital to analog and vice visa.

- **Data Acquisition Card**

It converts the analog signal that comes from the sensors (in our case) into digital signal that can be read by the computer.

✓ **Analog output (D/A converter)**

It converts digital signals to analog signals, for example, it converts signals from computer to the real word.

✓ **Digital input/output**

Digital input /output subsystems are designed to input and output digital values (logic levels) to and from hardware.

✓ **Counter /Timer subsystem**

It is used for event counting, frequency and period measurement and pulse train generation. The following figure shows us a DAQ hardware system

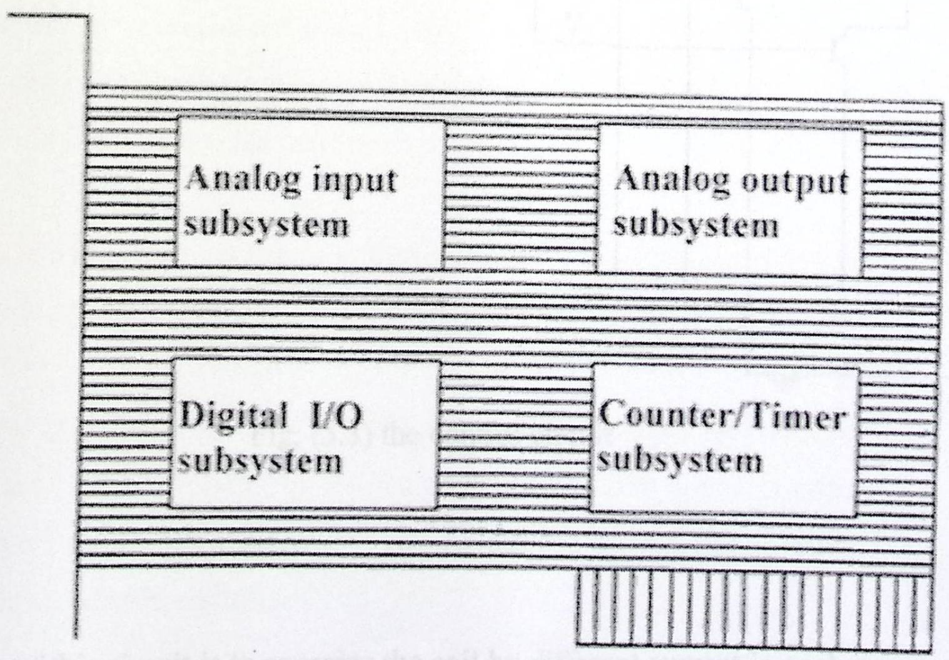

Fig. (5.2) Data acquisition card (DAQ)

We select the value of the loading into the program and when operate this program this value to the DAQ which convert it from digital to analog; and this value reach the opto-coupler it operate and the photo-diode which generate a pulse to the transistor to pass a signal to the main transistor to pass a current from it to energize the coil which make a opposite torque on the disc (motor).

5.3 CONTROL CIRCUIT

After study we select the following circuit to control and operate the driving circuit under the condition of the loading value which coming from the program (PC).

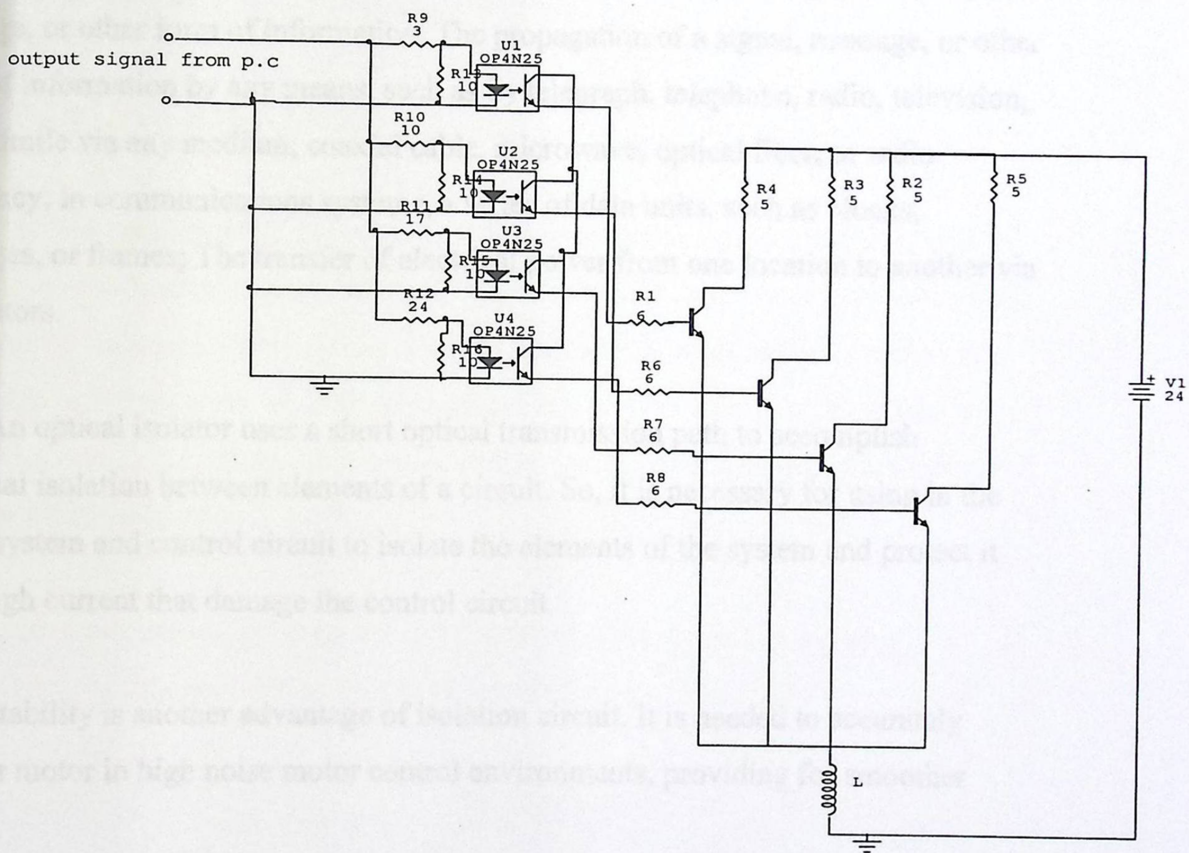

Fig. (5.3) the control circuit

The aim of this circuit is to energize the coil by different current in each we change the signal volt from P.C .

This circuit contains the following parameters:

- **Isolation Circuits:**

Optical isolator is a device that uses a short optical transmission path to accomplish electrical isolation between elements of a circuit. The optical path may be air or a dielectric waveguide. The transmitting and receiving elements of an optical isolator may be contained within a single compact module.

The optical isolator has many functions such as the dispatching of a signal, message, or other form of information; The propagation of a signal, message, or other form of information by any means, such as by telegraph, telephone, radio, television, or facsimile via any medium, coaxial cable, microwave, optical fiber, or radio frequency, in communications systems, a series of data units, such as blocks, messages, or frames; The transfer of electrical power from one location to another via conductors.

An optical isolator uses a short optical transmission path to accomplish electrical isolation between elements of a circuit. So, it is necessary for using in the motor system and control circuit to isolate the elements of the system and protect it from high current that damage the control circuit.

Stability is another advantage of isolation circuit. It is needed to accurately monitor motor in high noise motor control environments, providing for smoother control.

In various types of motor control applications, high accuracy and linearity are paramount under transient conditions. So, we must use isolation circuit between motor and control circuit, between control circuit and microprocessor, between microprocessor and power circuit.

- **MOSFET**

We used the MOSFT transistor in power circuit because of its characteristics. It is used as power switch and it has very high speed to turn on and off. Also, it rates very high currents reaches 50A.

5.4 DRIVING CIRCUIT.

The driving circuit in this project is the coil which energized by the dc current and produced the magnetic field which effect on the rotating disc and produce the opposite braking torque on it and loaded the motor.

5.5 TACHOGENERATOR:

An electromechanical generator is a device capable of producing electrical power from mechanical energy. When not connected to a load resistance, generators will generate voltage roughly proportional to shaft speed. With precise construction and design, generators can be built to produce very precise voltages for certain ranges of shaft speeds, thus making them well-suited as measurement devices for shaft speed in mechanical equipment.

A generator specially designed and constructed for this use is called a tachometer or tachogenerator as shown in figure (5.4).

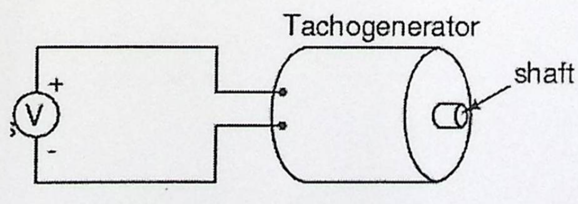

Figure (5.4): Tachogenerator diagram

By measuring the voltage produced by a tachogenerator, you can easily determine the rotational speed of whatever it's mechanically attached to. One of the more common voltage signal ranges used with tachogenerators is 0 to 10 volts. Obviously, since a tachogenerator cannot produce voltage when it's not turning, the zero cannot be "live" in this signal standard. Tachogenerators can be purchased with different "full-scale" (10 volt) speeds for different applications.

5.6 flow chart

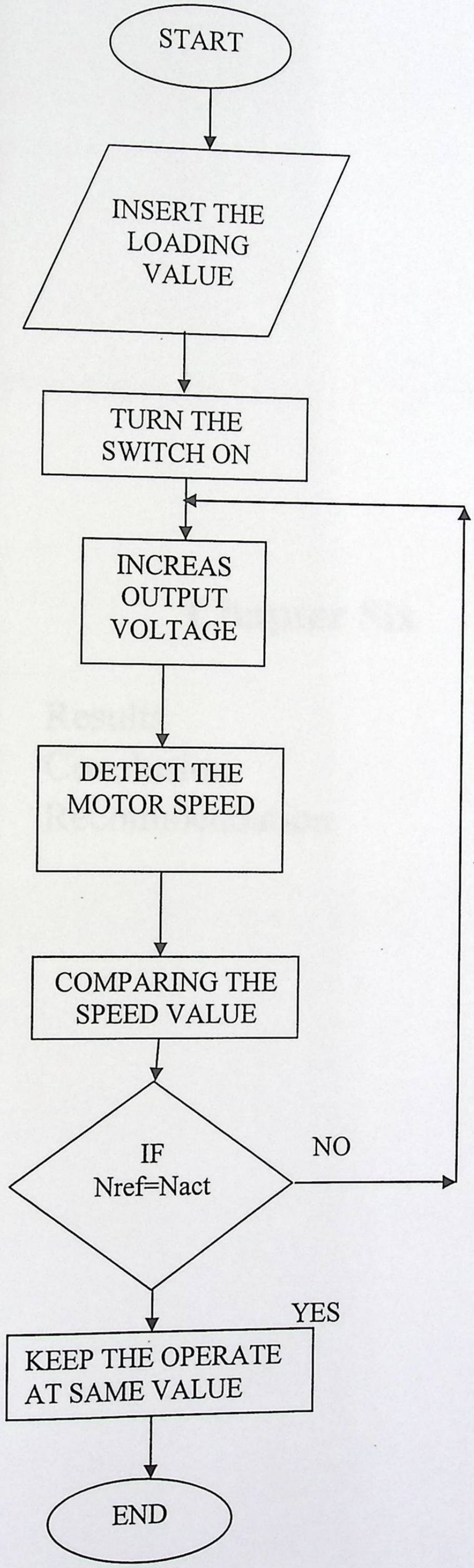

Chapter Six

- Results.
- Conclusion
- Recommendation

6.1 Result:

We use separately dc motor to load it by us load unit, the nominal plate of this motor is as follow:

Power: 0.1KW,

Armature current = 0.63A,

Speed = 2000 r.p.m,

Armature resistance = 56 Ω ,

We want show the effect of us unit on this motor and studying the characteristics of this motor using us load unit .

We loaded this motor at two cases:

Case 1: the rotation disc at this unit is iron disc at different air gap.

1- At air gap g = 3mm

I(braking) A	Va V	Ia A	If A	N Rpm	T N. m	ω 1/s	Pin W	Pout W	η %
0	220	0.23	.075	2255	0.2	236	67	47.76	71.3
1	220	0.29	.075	2225	0.26	233	80.3	59.46	74
2	220	0.33	.075	2200	0.3	230	89.1	66.8	75
2.5	220	0.35	.075	2190	0.31	229	93.5	70.5	75.4
3.2	220	0.4	.075	2175	0.35	227	104.5	80	76.6
4	220	0.42	.075	2165	0.37	226	108.9	83.5	76.7
4.5	220	0.45	.075	2140	0.4	224	115.5	88.7	76.8

Table (6.1) measurement and calculated data for iron disc at air gap 3mm

2- At air gab g = 6mm.

I(braking) A	Va V	Ia A	If A	N Rpm	T N.m	ω 1/s	Pin W	Pout W	η %
0	220	0.22	.075	2240	0.19	237	65	45.88	70.5
1	220	0.25	.075	2230	0.22	233	71.5	51.26	71.7
2	220	0.26	.075	2225	0.23	232.8	73.7	53.26	72.3
2.5	220	0.26	.075	2225	0.23	232.8	73.7	53.26	72.3
3.2	220	0.28	.075	2225	0.25	232.2	73.7	58	78.7
4.5	220	0.35	.075	2225	0.31	232	93.5	71.45	76.4

Table (6.2) measurement and calculated data for iron disc at air gap 6mm

Case 2: the rotation disc at this unit is aluminum disc at different air gap

1- At air gab g = 3mm

I(braking) A	Va V	Ia A	If A	N Rpm	T N.m	ω 1/s	Pin W	Pout W	η %
0	220	0.25	.075	2240	0.22	234.4	71.5	51.6	72
1	220	0.29	.075	2220	0.25	232.3	80.3	59.3	73.8
2	220	0.34	.075	2190	0.3	229.2	91.3	68.5	75.1
2.5	220	0.37	.075	2185	0.32	228.7	98	74.5	76
3.2	220	0.41	.075	2165	0.36	226.6	106.7	81.7	76.6
4	220	0.44	.075	2150	0.38	225	113.3	87	76.9
4.5	220	0.46	.075	2140	0.4	224	117.7	90.6	77

Table (6.3) measurement and calculated data for aluminum disc at air gap 3mm.

2 - At air gab g = 6mm

I(braking) A	Va V	Ia A	If A	N Rpm	T N.m	ω 1/s	Pin W	Pout	η %
0	220	0.24	.075	2240	0.21	234.4	69.3	49.5	71.4
1	220	0.28	.075	2238	0.24	234.2	78.1	57.7	73.8
2	220	0.3	.075	2225	0.26	232.8	82.5	61.5	74.5
2.5	220	0.33	.075	2218	0.3	232.1	89.1	67.4	75.6
3.2	220	0.35	.075	2200	0.31	230.2	93.5	71	75.8
4	220	0.38	.075	2185	0.33	228.6	100	76.4	76.4
4.5	220	0.39	.075	2175	0.34	227.6	102.3	78.1	76.3

Table (6.4) measurement and calculated data for aluminum disc at air gap 6mm.

The equation that used in calculated data is: (the calculated data is at neglecting ftriction and windage torque)

CALCULATING "ω":

$$\omega = (2\pi/60)*n$$

where:

n : the speed of motor.

CALCULATING TORQUE:

$$T = C\Phi I_a$$

Where :

T : is the electrical torque and it is equle output mechanical torque (by neglecing ftriction and windage torque)

$$C\Phi = (V_a - I_aR_a)/\ \omega$$

$= (220 - 0.63*56\ )/\ (2\pi/60)*2000 = 0.88$

CALCULATING INPUT POWER:

$$P_{in} = V_a\ I_a + V_f I.f$$

Where:

Va:armature voltge of the motor.

Ia: armature current of the motor .

Vf:filde votage of the motor and its equle Va.

If : filde current of the motor and it is conctant .

CALCULATING OUTPUT POWER:

$$Pout = T. \omega$$

CALCULATING THE EFFICIENCY:

$$\eta\% = (Pout/ Pin)*100$$

THE RELATION BETWEEN BRAKING CURRENT AND MOTOR TORQUE AT DIFFERENT CASES

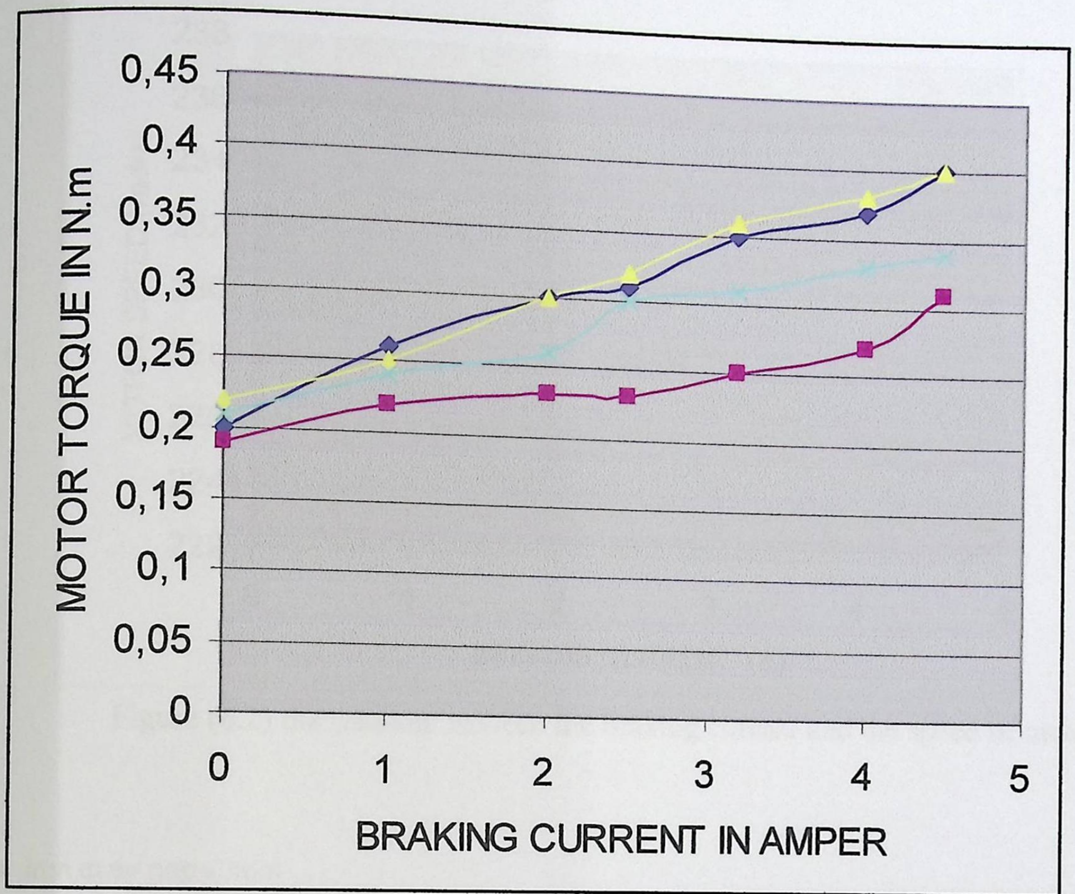

Figure (6.1) the relation between the motor torque and the braking current

- iron at air gap = 3mm.
- iron at air gap = 6mm
- aluminum at air gap = 3mm.
- aluminum at air gap = 6mm.

From this figure we show that as the braking current (the current that energiz the coil) increas the motor torque increas , for disc at air gap 3mm the motor torque is hight than motor torque for the same disc at air gap 6mm ; it mean that as air gap increas the loading is eddy current on the disc is decreas so the braking torque on the disc is decreas , also for a diffeint discs (at same braking current and same air gap) the loading on aluminum disc is bettar than on iron disc ; it mean the eddy current form large on a disc that have the hight resistevaty .

THE RELATION BETWEEN BRAKING CURRENT AND MOTOR SPEED AT DIFFERANT CASES

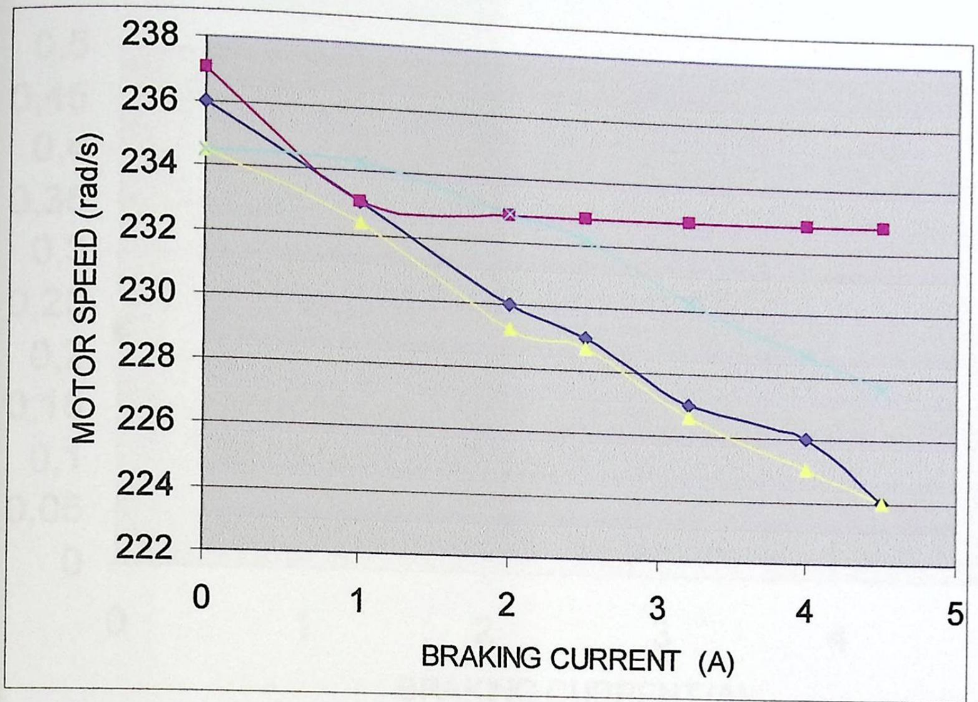

Figure (6.2) the relation between the braking current and the speed of motor

- iron at air gap = 3mm.
- iron at air gap = 6mm
- aluminum at air gap = 3mm.
- aluminum at air gap = 6mm.

From this figure we show that as braking current increase the motor speed is decrease

THE RELATION BETWEEN BRAKING CURRENT AND MOTOR TORQUE AT DIFFERENT CASES

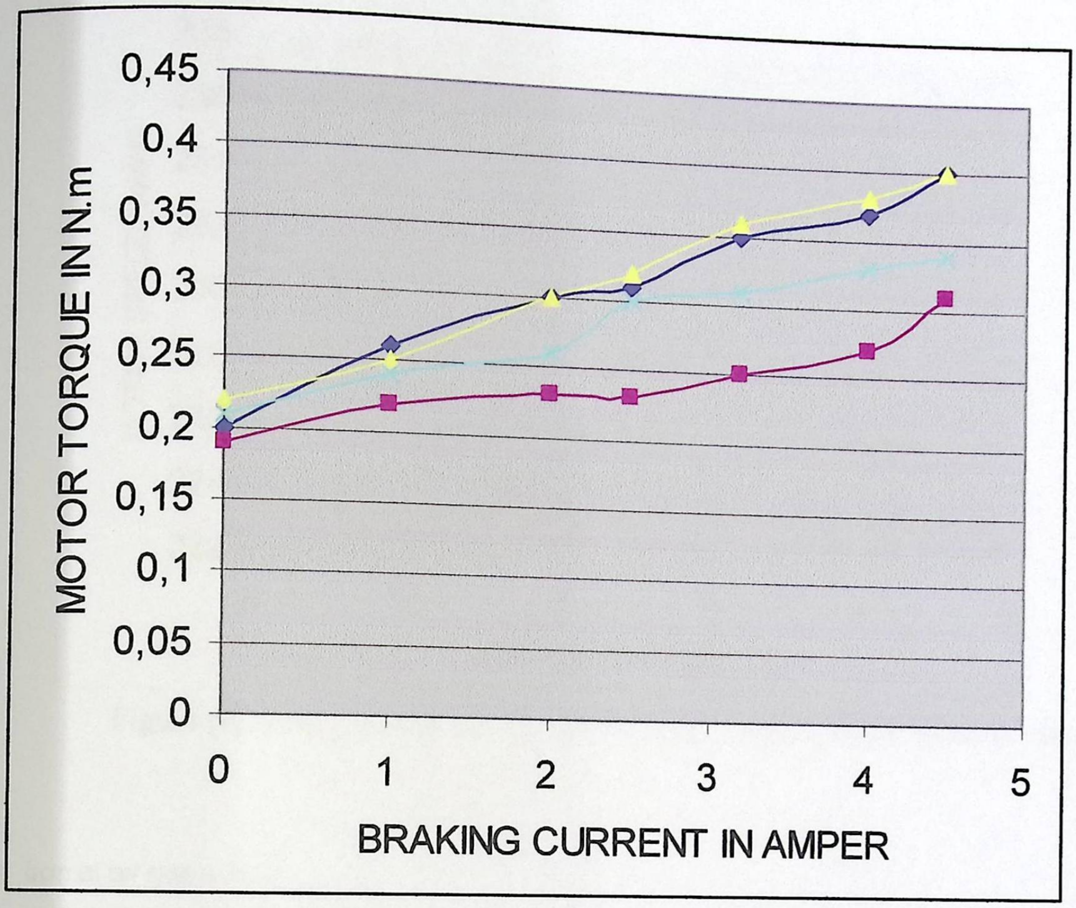

Figure (6.1) the relation between the motor torque and the braking current

- iron at air gap = 3mm.
- iron at air gap = 6mm
- aluminum at air gap = 3mm.
- aluminum at air gap = 6mm.

From this figure we show that as the braking current (the current that energiz the coil) increas the motor torque increas , for disc at air gap 3mm the motor torque is hight than motor torque for the same disc at air gap 6mm ; it mean that as air gap increas the loading is eddy current on the disc is decreas so the braking torque on the disc is decreas , also for a diffeint discs (at same braking current and same air gap) the loading on aluminum disc is bettar than on iron disc ; it mean the eddy current form large on a disc that have the hight resistevaty .

THE RELATION BETWEEN BRAKING CURRENT AND MOTOR CURRENT AT DIFFERANT CASE

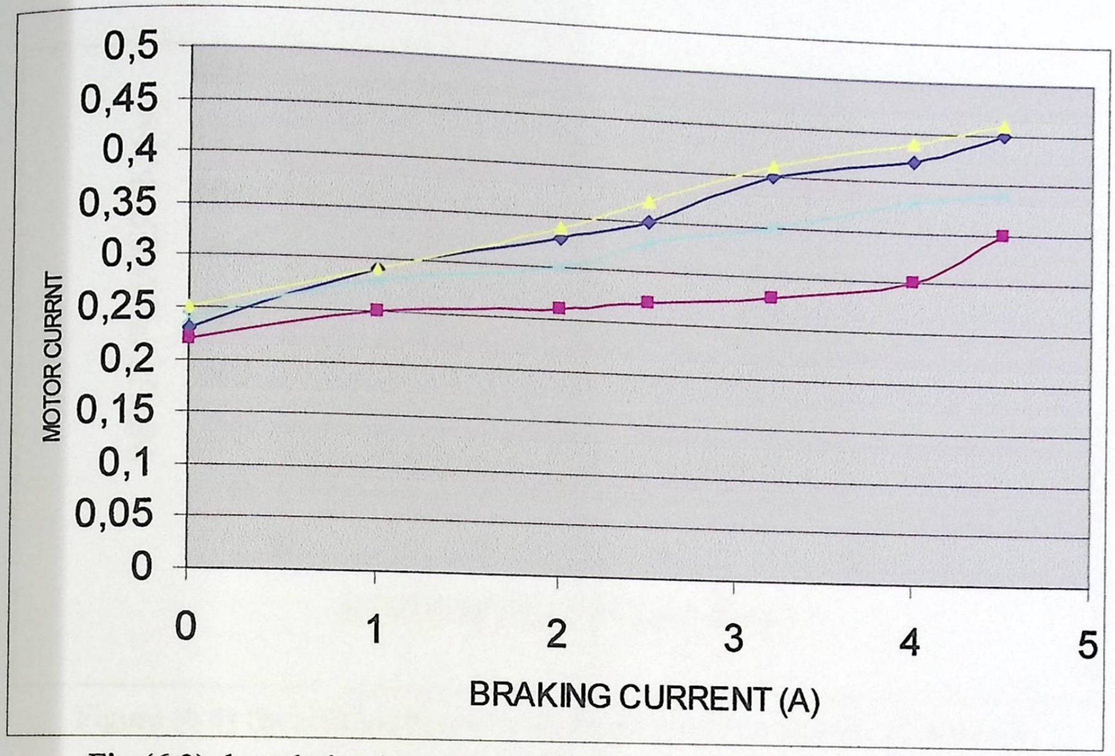

Fig (6.3) the relation between the braking current and the motor current

- iron at air gap = 3mm.
- iron at air gap = 6mm
- aluminum at air gap = 3mm.
- aluminum at air gap = 6mm.

from this figuer we show that as braking current increas the motor current will increas .

THE RELATION BETWEEN THE BRAKING CURRENT AND INPUT POWER FOR DIFFERANT CASES.

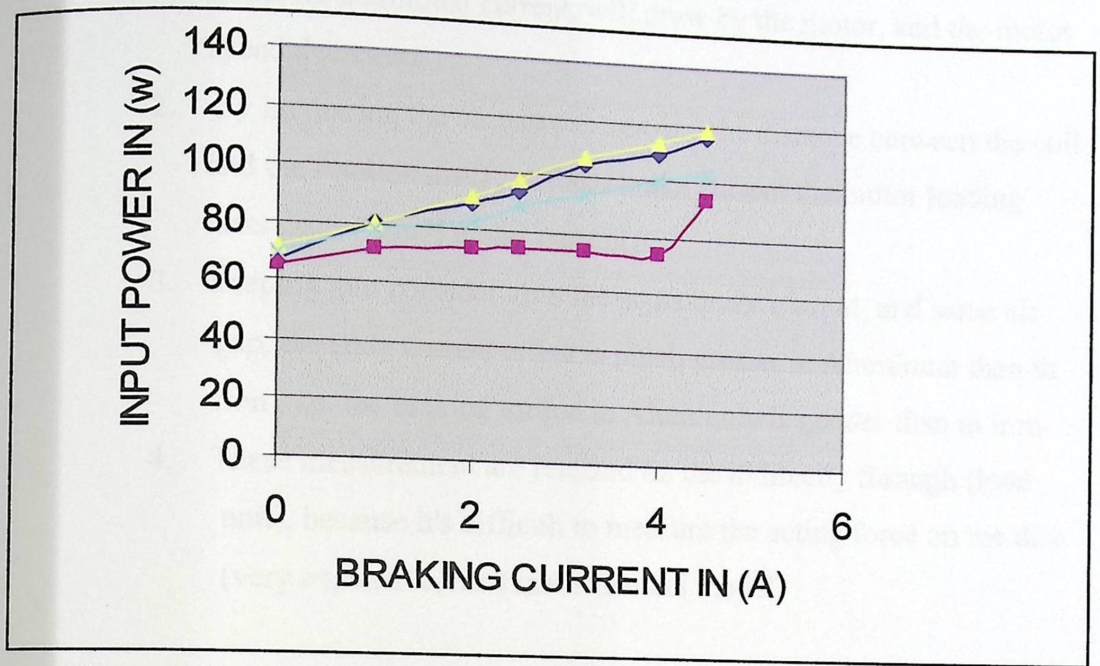

Figure (6.4) the relation between the braking current and the input power.

- iron at air gap = 3mm.
- iron at air gap = 6mm
- aluminum at air gap = 3mm.
- aluminum at air gap = 6mm.

From this figure we show that as braking current increase the input power increase.

6.2 CONCLUSION:

1. By increasing the brake current, the loading torque increases therefore additional current, will draw by the motor, and the motor speed decreases
2. By increasing the air gap (increasing the distance between the coil and the rotation disc) , at fixed brake current the motor loading decreases (small motor current).
3. keeping into consideration the same brake current, and same air gap, the eddy current effect is much greater in Aluminum than in iron , i.e. the braking torque in Aluminum is greater than in iron.
4. These measurement are realized on the indirectly through (load unit), because it's difficult to measure the acting force on the disc (very expensive, hard mathematical model.

6.3 RECOMEDATION

1. Comparable analysis between aluminum and copper may be done and compar at with us result.
2. the electromagnetic loading unit suitable for this system may be design in the future.
3. further attention to learning the student in using P.C technics (e.g DAQ technics) and applying at in motor control.

Appendix

- appendix A
- appendix B
- appendix C
- appendix D

Appendix A

DATA SHEETS

International
IOR Rectifier

PD - 94004A

IRFP260N

HEXFET® Power MOSFET

- Advanced Process Technology
- Dynamic dv/dt Rating
- 175°C Operating Temperature
- Fast Switching
- Fully Avalanche Rated
- Ease of Paralleling
- Simple Drive Requirements

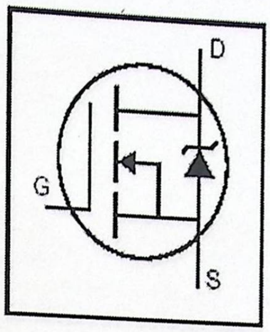

V_{DSS} = 200V

$R_{DS(on)}$ = 0.04Ω

I_D = 50A

Description

Fifth Generation HEXFETs from International Rectifier utilize advanced processing techniques to achieve extremely low on-resistance per silicon area. This benefit, combined with the fast switching speed and ruggedized device design that HEXFET Power MOSFETs are well known for, provides the designer with an extremely efficient and reliable device for use in a wide variety of applications.

The TO-247 package is preferred for commercial-industrial applications where higher power levels preclude the use of TO-220 devices. The TO-247 is similar but superior to the earlier TO-218 package because of its isolated mounting hole.

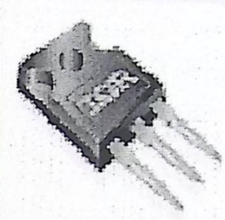

TO-247AC

Absolute Maximum Ratings

	Parameter	Max.	Units
I_D @ T_C = 25°C	Continuous Drain Current, V_{GS} @ 10V	50	A
I_D @ T_C = 100°C	Continuous Drain Current, V_{GS} @ 10V	35	
I_{DM}	Pulsed Drain Current ①	200	
P_D @ T_C = 25°C	Power Dissipation	300	W
	Linear Derating Factor	2.0	W/°C
V_{GS}	Gate-to-Source Voltage	±20	V
E_{AS}	Single Pulse Avalanche Energy②	560	mJ
I_{AR}	Avalanche Current①	50	A
E_{AR}	Repetitive Avalanche Energy①	30	mJ
dv/dt	Peak Diode Recovery dv/dt ③	10	V/ns
T_J T_{STG}	Operating Junction and Storage Temperature Range	-55 to +175	°C
	Soldering Temperature, for 10 seconds	300 (1.6mm from case)	
	Mounting torque, 6-32 or M3 srew	10 lbf•in (1.1N•m)	

Thermal Resistance

	Parameter	Typ.	Max.	Units
$R_{θJC}$	Junction-to-Case	—	0.50	°C/W
$R_{θCS}$	Case-to-Sink, Flat, Greased Surface	0.24	—	
$R_{θJA}$	Junction-to-Ambient	—	40	

International
IOR Rectifier

PD - 94004A

IRFP260N

HEXFET® Power MOSFET

- Advanced Process Technology
- Dynamic dv/dt Rating
- 175°C Operating Temperature
- Fast Switching
- Fully Avalanche Rated
- Ease of Paralleling
- Simple Drive Requirements

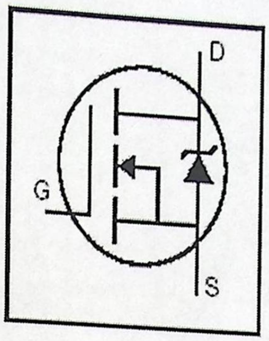

V_{DSS} = 200V

$R_{DS(on)}$ = 0.04Ω

I_D = 50A

Description

Fifth Generation HEXFETs from International Rectifier utilize advanced processing techniques to achieve extremely low on-resistance per silicon area. This benefit, combined with the fast switching speed and ruggedized device design that HEXFET Power MOSFETs are well known for, provides the designer with an extremely efficient and reliable device for use in a wide variety of applications.

The TO-247 package is preferred for commercial-industrial applications where higher power levels preclude the use of TO-220 devices. The TO-247 is similar but superior to the earlier TO-218 package because of its isolated mounting hole.

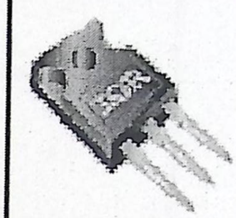

TO-247AC

Absolute Maximum Ratings

	Parameter	Max.	Units
I_D @ T_C = 25°C	Continuous Drain Current, V_{GS} @ 10V	50	A
I_D @ T_C = 100°C	Continuous Drain Current, V_{GS} @ 10V	35	
I_{DM}	Pulsed Drain Current ①	200	
P_D @T_C = 25°C	Power Dissipation	300	W
	Linear Derating Factor	2.0	W/°C
V_{GS}	Gate-to-Source Voltage	±20	V
E_{AS}	Single Pulse Avalanche Energy②	560	mJ
I_{AR}	Avalanche Current①	50	A
E_{AR}	Repetitive Avalanche Energy①	30	mJ
dv/dt	Peak Diode Recovery dv/dt ③	10	V/ns
T_J T_{STG}	Operating Junction and Storage Temperature Range	-55 to +175	°C
	Soldering Temperature, for 10 seconds	300 (1.6mm from case)	
	Mounting torque, 6-32 or M3 srew	10 lbf•in (1.1N•m)	

Thermal Resistance

	Parameter	Typ.	Max.	Units
$R_{θJC}$	Junction-to-Case	—	0.50	°C/W
$R_{θCS}$	Case-to-Sink, Flat, Greased Surface	0.24	—	
$R_{θJA}$	Junction-to-Ambient	—	40	

IRFP260N

International
IOR Rectifier

Electrical Characteristics @ $T_J = 25°C$ (unless otherwise specified)

	Parameter	Min.	Typ.	Max.	Units	Conditions
$V_{(BR)DSS}$	Drain-to-Source Breakdown Voltage	200	—	—	V	$V_{GS} = 0V$, $I_D = 250\mu A$
$\Delta V_{(BR)DSS}/\Delta T_J$	Breakdown Voltage Temp. Coefficient	—	0.26	—	V/°C	Reference to 25°C, $I_D = 1mA$
$R_{DS(on)}$	Static Drain-to-Source On-Resistance	—	—	0.04	Ω	$V_{GS} = 10V$, $I_D = 28A$ ④
$V_{GS(th)}$	Gate Threshold Voltage	2.0	—	4.0	V	$V_{DS} = V_{GS}$, $I_D = 250\mu A$
g_{fs}	Forward Transconductance	27	—	—	S	$V_{DS} = 50V$, $I_D = 28A$ ④
I_{DSS}	Drain-to-Source Leakage Current	—	—	25	μA	$V_{DS} = 200V$, $V_{GS} = 0V$
		—	—	250		$V_{DS} = 160V$, $V_{GS} = 0V$, $T_J = 150°C$
I_{GSS}	Gate-to-Source Forward Leakage	—	—	100	nA	$V_{GS} = 20V$
	Gate-to-Source Reverse Leakage	—	—	-100		$V_{GS} = -20V$
Q_g	Total Gate Charge	—	—	234	nC	$I_D = 28A$
Q_{gs}	Gate-to-Source Charge	—	—	38		$V_{DS} = 160V$
Q_{gd}	Gate-to-Drain ("Miller") Charge	—	—	110		$V_{GS} = 10V$ ④
$t_{d(on)}$	Turn-On Delay Time	—	17	—	ns	$V_{DD} = 100V$
t_r	Rise Time	—	60	—		$I_D = 28A$
$t_{d(off)}$	Turn-Off Delay Time	—	55	—		$R_G = 1.8\Omega$
t_f	Fall Time	—	48	—		$V_{GS} = 10V$ ④
L_D	Internal Drain Inductance	—	5.0	—	nH	Between lead, 6mm (0.25in.) from package 
L_S	Internal Source Inductance	—	13	—		and center of die contact
C_{iss}	Input Capacitance	—	4057	—	pF	$V_{GS} = 0V$
C_{oss}	Output Capacitance	—	603	—		$V_{DS} = 25V$
C_{rss}	Reverse Transfer Capacitance	—	161	—		$f = 1.0MHz$

Source-Drain Ratings and Characteristics

	Parameter	Min.	Typ.	Max.	Units	Conditions
I_S	Continuous Source Current (Body Diode)	—	—	50	A	MOSFET symbol showing the 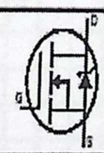
I_{SM}	Pulsed Source Current (Body Diode)①	—	—	200		integral reverse p-n junction diode.
V_{SD}	Diode Forward Voltage	—	—	1.3	V	$T_J = 25°C$, $I_S = 28A$, $V_{GS} = 0V$ ④
t_{rr}	Reverse Recovery Time	—	268	402	ns	$T_J = 25°C$, $I_F = 28A$
Q_{rr}	Reverse Recovery Charge	—	1.9	2.8	μC	$di/dt = 100A/\mu s$ ④
t_{on}	Forward Turn-On Time	Intrinsic turn-on time is negligible (turn-on is dominated by L_S+L_D)				

Notes:

① Repetitive rating; pulse width limited by max. junction temperature.

② Starting $T_J = 25°C$, $L = 1.5mH$ $R_G = 25\Omega$, $I_{AS} = 28A$.

③ $I_{SD} \le 28A$, $di/dt \le 486A/\mu s$, $V_{DD} \le V_{(BR)DSS}$, $T_J \le 175°C$

④ Pulse width ≤ 400μs; duty cycle ≤ 2%.

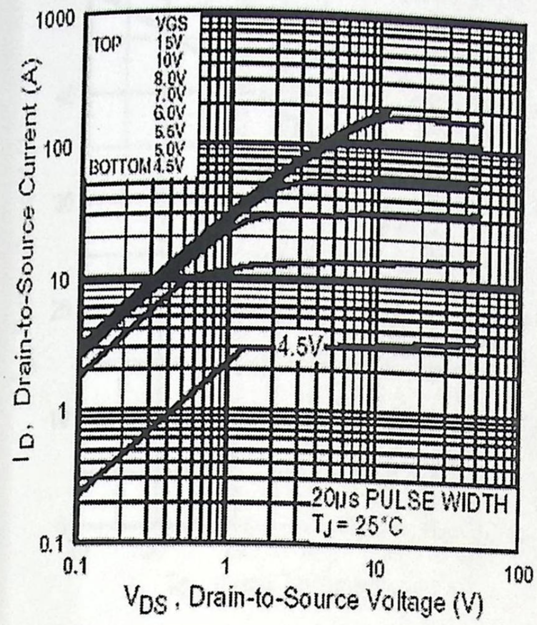

Fig 1. Typical Output Characteristics

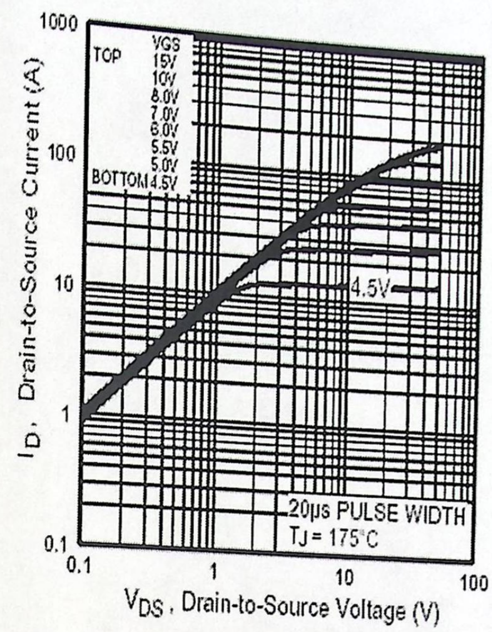

Fig 2. Typical Output Characteristics

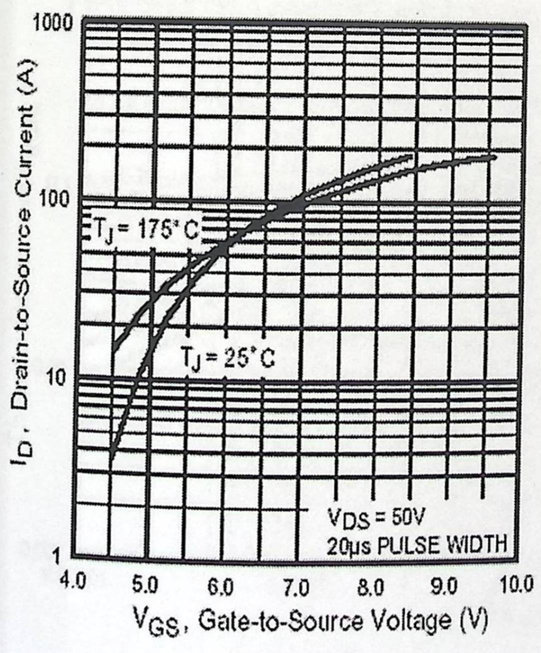

Fig 3. Typical Transfer Characteristics

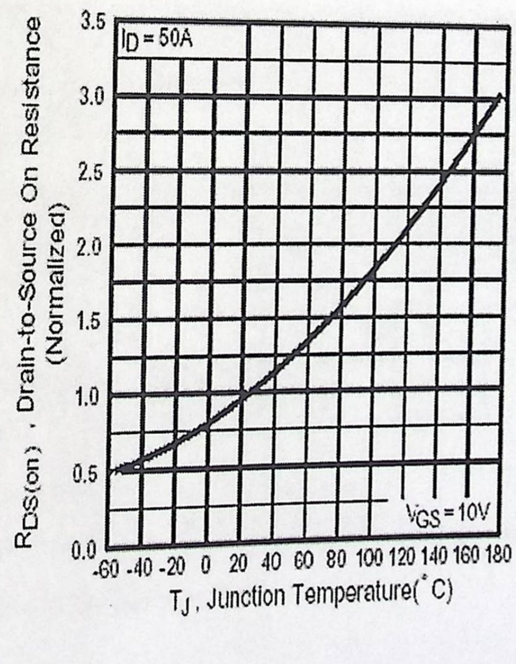

Fig 4. Normalized On-Resistance Vs. Temperature

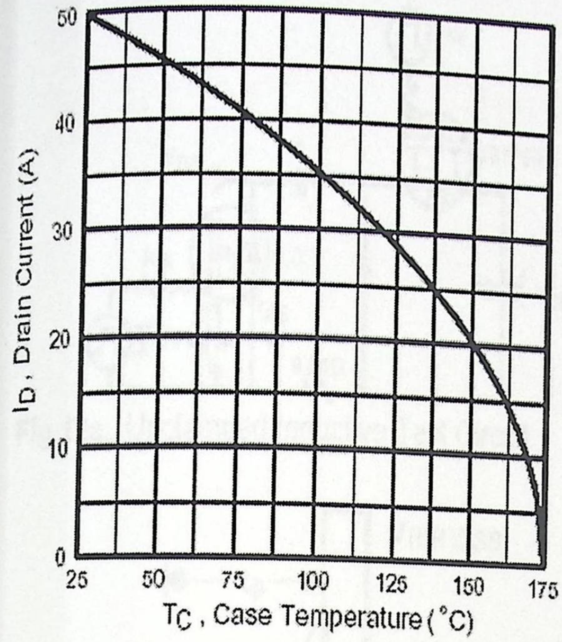

Fig 9. Maximum Drain Current Vs. Case Temperature

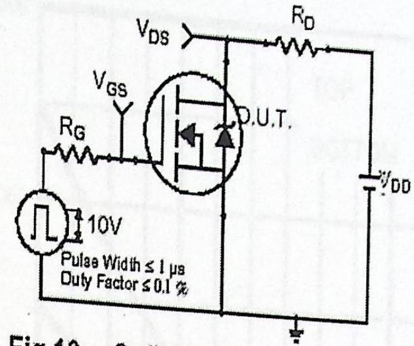

Fig 10a. Switching Time Test Circuit

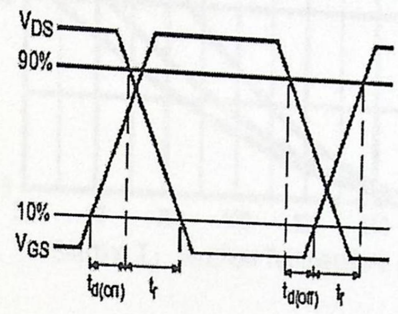

Fig 10b. Switching Time Waveforms

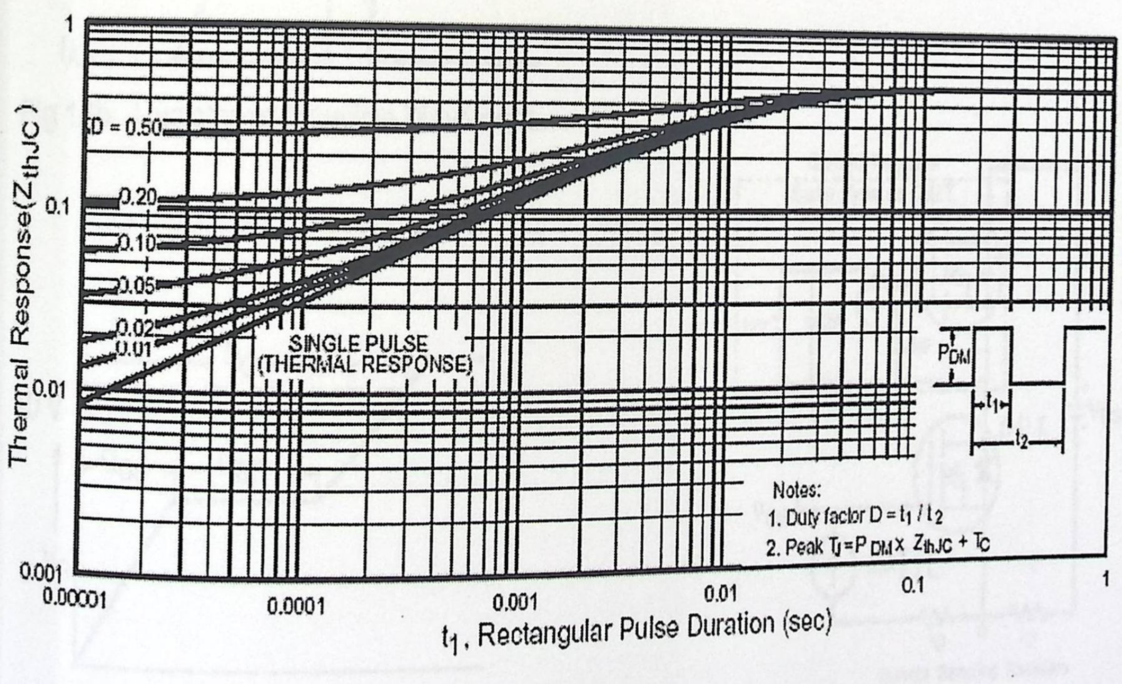

Fig 11. Maximum Effective Transient Thermal Impedance, Junction-to-Case

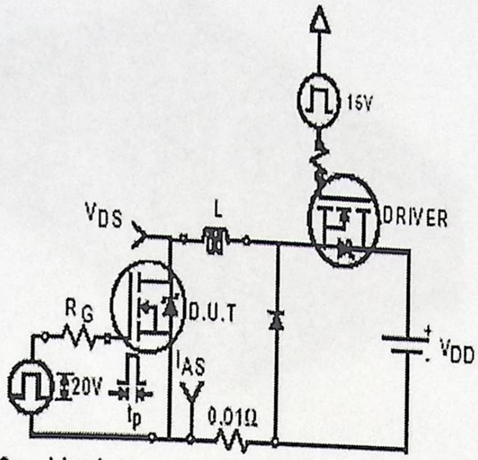

Fig 12a. Unclamped Inductive Test Circuit

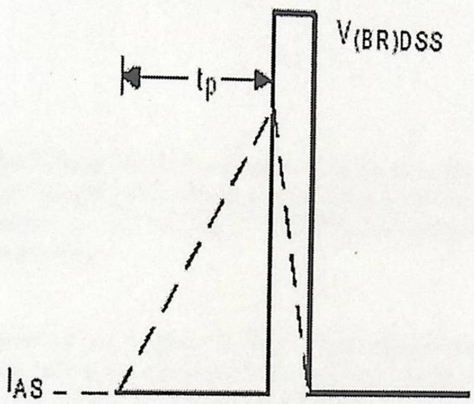

Fig 12b. Unclamped Inductive Waveforms

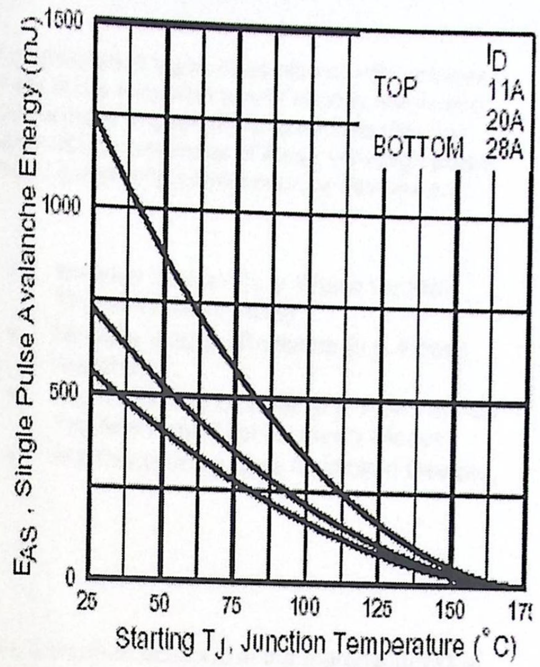

Fig 12c. Maximum Avalanche Energy Vs. Drain Current

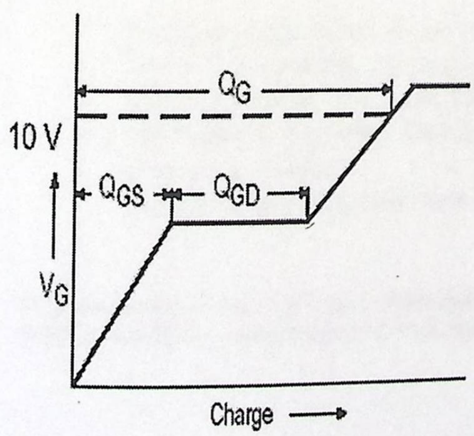

Fig 13a. Basic Gate Charge Waveform

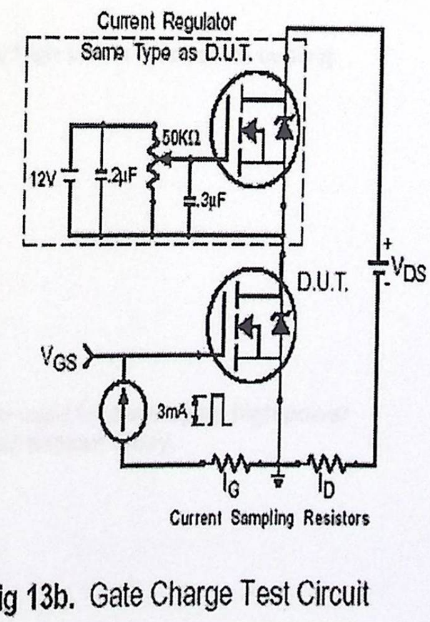

Fig 13b. Gate Charge Test Circuit

High Power Heat Sinks

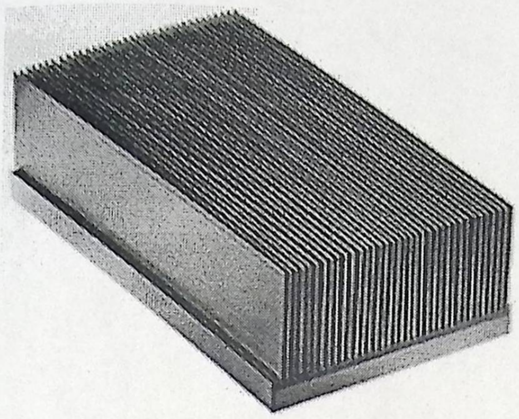

Many specialized types of semiconductor devices operate at the very high power density levels and require a more engineered and intense thermal solution. Some examples of these very high power density / generating semiconductor devices are:

- Rectifier Devices (e.g. Phase Control Thyristors and Diodes)
- Medium Voltage Thyristors (e.g. Power Switches)
- Fast Switching Devices (e.g. Fast Turn-off Thyristors and Fast Recovery Diodes)
- IGBT's including Gate Controlled Devices,

GTO Thyristors

The industrial use of these products is quite versatile. Industries engaged in the manufacturing of electric vehicles, telecommunications, military, aerospace, welding equipment, motor controls, traction drive, and HVDC require a cooling solution specific to each design and ultimate power dissipation.

ThermaFlo develops efficient cooling solution for these industries using a methodology of applying standard product manufacturing technology and know-how towards developing a cooling solution for cooling high power electronics.

Some of the technologies that ThermaFlo uses in developing high power electronics cooling systems are:

- Extremely High Aspect Ratio Heat sink Extrusions
- Folded Fin Heat sink Technology
- Bonded Fin Heat sink Technology
- High Mass and Surface Area Extruded Heat sink
- Copper Heat sinks
- Integrated Heat Pipe and Heat Sink Solutions

To learn more about these and other technologies that can be used for developing high power cooling solutions, please contact ThermaFlo's Engineering Department today.

RATINGS AND CHARACTERISTIC CURVES (BY396 THRU BY399)

FIG.1- MAXIMUM FORWARD CURRENT DERATING CURVE

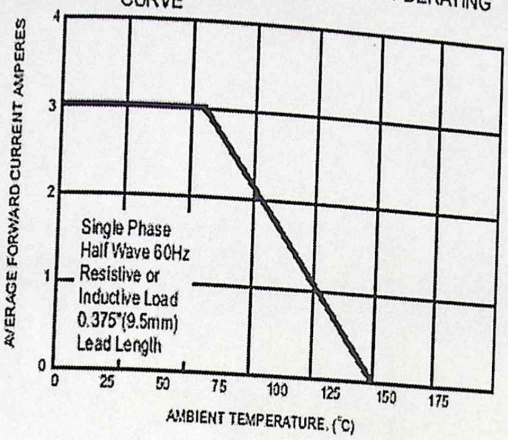

FIG.2- MAXIMUM NON-REPETITIVE PEAK FORWARD SURGE CURRENT

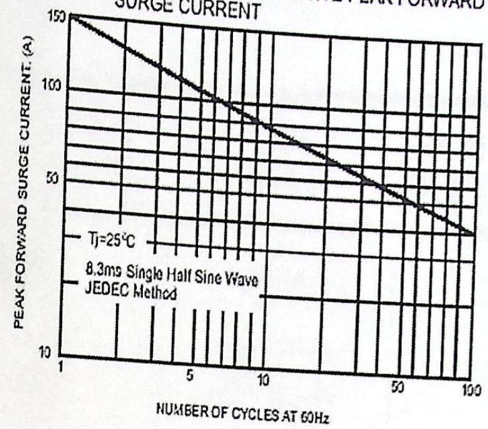

FIG.3- TYPICAL FORWARD CHARACTERISTICS

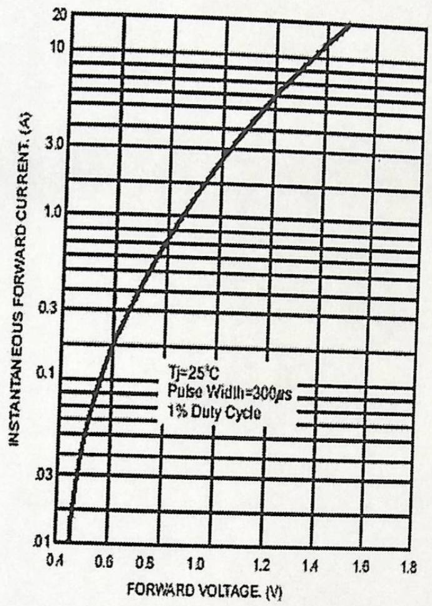

FIG.4- TYPICAL JUNCTION CAPACITANCE

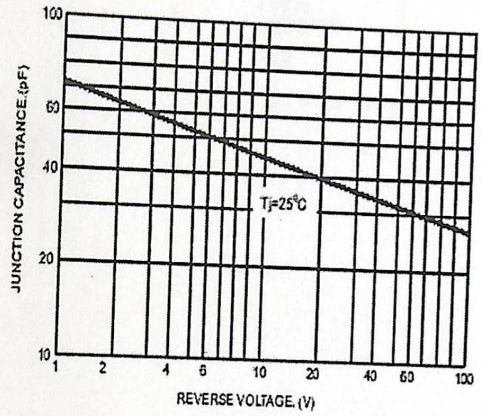

FIG.5- REVERSE RECOVERY TIME CHARACTERISTIC AND TEST CIRCUIT DIAGRAM

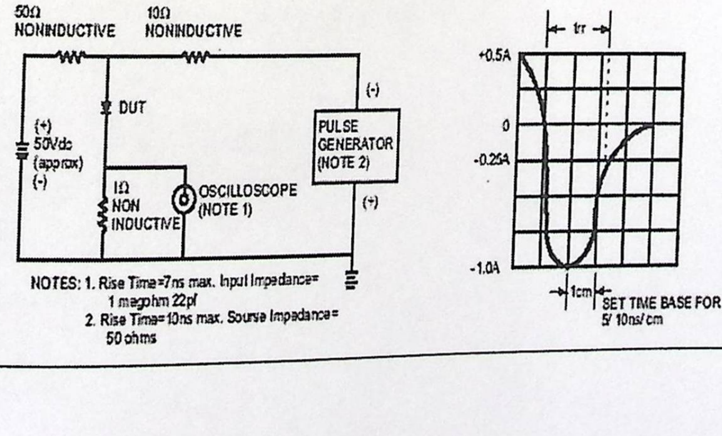

FAIRCHILD SEMICONDUCTOR®

GENERAL PURPOSE 6-PIN PHOTOTRANSISTOR OPTOCOUPLERS

4N25	4N26	4N27	4N28	4N35	4N36
4N37	H11A1	H11A2	H11A3	H11A4	H11A5

WHITE PACKAGE (-M SUFFIX)

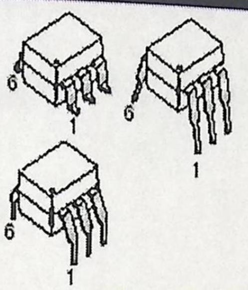

SCHEMATIC

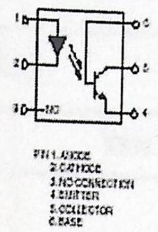

BLACK PACKAGE (NO -M SUFFIX)

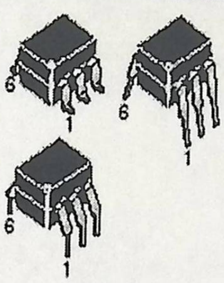

DESCRIPTION

The general purpose optocouplers consist of a gallium arsenide infrared emitting diode driving a silicon phototransistor in a 6-pin dual in-line package.

FEATURES

- Also available in white package by specifying -M suffix, eg. 4N25-M
- UL recognized (File # E90700)
- VDE recognized (File # 94766)
  - Add option V for white package (e.g., 4N25V-M)
  - Add option 300 for black package (e.g., 4N25.300)

APPLICATIONS

- Power supply regulators
- Digital logic inputs
- Microprocessor inputs

FAIRCHILD SEMICONDUCTOR®

GENERAL PURPOSE 6-PIN PHOTOTRANSISTOR OPTOCOUPLERS

4N25	4N26	4N27	4N28	4N35	4N36
4N37	H11A1	H11A2	H11A3	H11A4	H11A5

ABSOLUTE MAXIMUM RATINGS (T_A = 25°C unless otherwise specified)

Parameter	Symbol	Value	Units
TOTAL DEVICE			
Storage Temperature	T_{STG}	-55 to +150	°C
Operating Temperature	T_{OPR}	-55 to +100	°C
Wave solder temperature (see page 14 for reflow solder profiles)	T_{SOL}	260 for 10 sec	°C
Total Device Power Dissipation @ T_A = 25°C	P_D	250	mW
Derate above 25°C		3.3 (non-M), 2.94 (-M)	
EMITTER			
DC/Average Forward Input Current	I_F	100 (non-M), 60 (-M)	mA
Reverse Input Voltage	V_R	6	V
Forward Current - Peak (300µs, 2% Duty Cycle)	$I_F(pk)$	3	A
LED Power Dissipation @ T_A = 25°C	P_D	150 (non-M), 120 (-M)	mW
Derate above 25°C		2.0 (non-M), 1.41 (-M)	mW/°C
DETECTOR			
Collector-Emitter Voltage	V_{CEO}	30	V
Collector-Base Voltage	V_{CBO}	70	V
Emitter-Collector Voltage	V_{ECO}	7	V
Detector Power Dissipation @ T_A = 25°C	P_D	150	mW
Derate above 25°C		2.0 (non-M), 1.76 (-M)	mW/°C

Fig. 19 Dark Current vs. Ambient Temperature

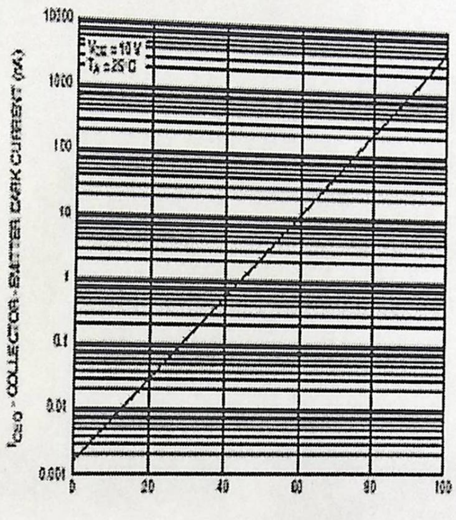

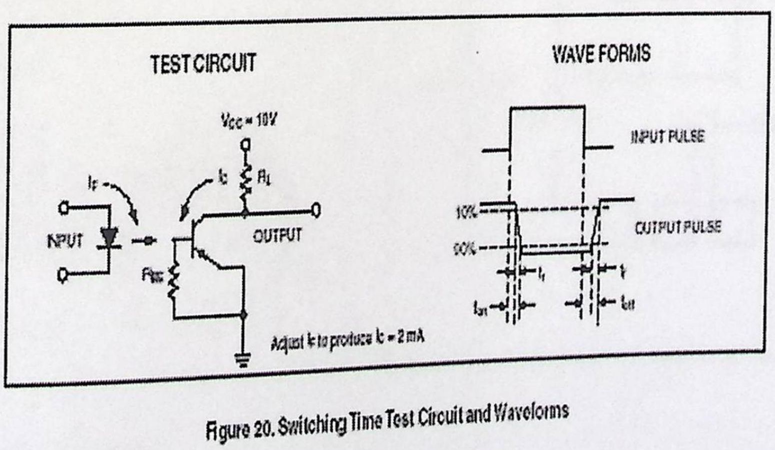

Figure 20. Switching Time Test Circuit and Waveforms

FAIRCHILD SEMICONDUCTOR®

GENERAL PURPOSE 6-PIN PHOTOTRANSISTOR OPTOCOUPLERS

4N25 4N37	4N26 H11A1	4N27 H11A2	4N28 H11A3	4N35 H11A4	4N36 H11A5

Black Package (No -M Suffix)

Package Dimensions (Through Hole)

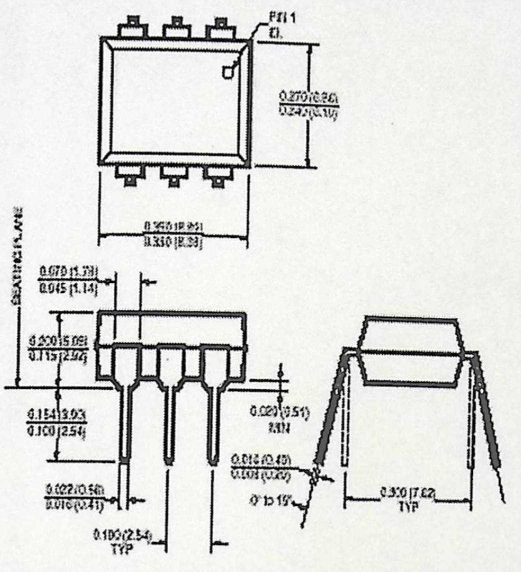

Package Dimensions (Surface Mount)

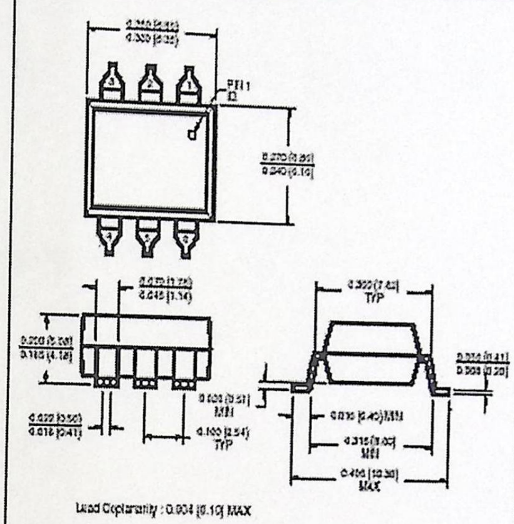

Package Dimensions (0.4" Lead Spacing)

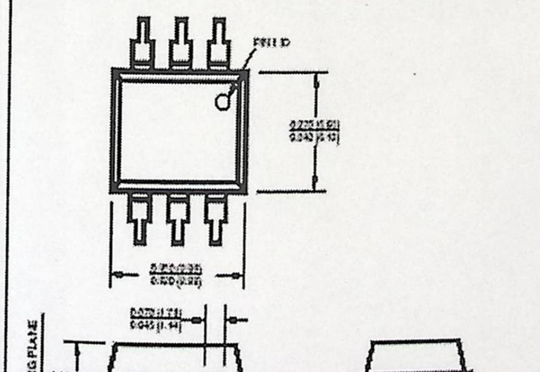

Recommended Pad Layout for Surface Mount Leadform

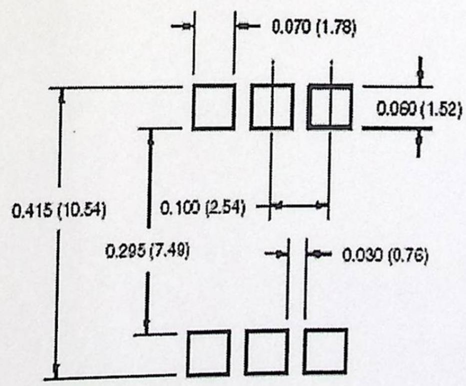

NOTE
All dimensions are in inches (millimeters)

Appendix B

Material constants

Table 1: gives the conductivity for a number of metallic

material	$\sigma, \Omega/m$	material	$\sigma, \Omega/m$
Silver	6.17×10^{7}	Graphite	7×10^{4}
Copper	5.8×10^{7}	Silicon	1200
Gold	4.1×10^{7}	Ferrite (typical)	100
Aluminum	3.82×10^{7}	Water (sea)	5
Tungsten	1.82×10^{7}	Limestone	10^{-2}
Zinc	1.67×10^{7}	Clay	5×10^{-3}
Brass	1.5×10^{7}	Water (fresh)	10^{-3}
Nickel	1.45×10^{7}	Water (distilled)	10^{-4}
Iron	1.03×10^{7}	Soil (sandy)	10^{-5}
Phosphor bronze	1.0×10^{7}	Granite	10^{-6}
Solder	0.7×10^{7}	Marble	10^{-8}
Carbon steel	0.6×10^{7}	Bakelite	10^{-9}
German silver	0.3×10^{7}	Porcelain (dry process)	10^{-10}
Managing	0.227×10^{7}	Diamond	2×10^{-13}
Constantan	0.226×10^{7}	Polystyrene	10^{-16}
Constanium	0.22×10^{7}	quartz	10^{-17}
Stainless steel	0.11×10^{7}		
Nichrome	0.1×10^{7}		

Table 2: gives the relative permeability for various diamagnetic , paramagnetic , ferromagnetic materials .

Material	μ_R
Bismuth	0.9999986
Paraffin	0.99999942
Wood	0.9999995
Silver	0.99999981
Aluminum	1.00000065
Beryllium	1.000000079
Nickel chloride	1.00004
Manganese sulfate	1.0001
Nickel	50
Cast iron	60
Cobalt	60
Powdered iron	100
Machine steel	300
Ferrite (typical)	1000
Permalloy 45	2500
Transformer iron	3000
Silicon iron	3500
Iron (pure)	4000
Mumetal	20000
Sendust	30000
Supermalloy	100000

Appendix C
Software program

```
#include<stdio.h>
#include<math.h>
#include<dos.h>
#include<conio.h>
#define base 0x320
main()
{
 float Vmeasured, desired, error, Vm;
 int v;
 do{
 outport(base+19,0x00);
 outport(base+20,0x00);
 outport(base+22,0x00);
 do
 {
  v=inport(base+21);
  v= v&0x01;
 }
 while(v!=0x00);
 Vmeasured=inport(base+22);
 Vm=10-5*Vmeasured/(0xc00-0x800);
 Vm= 10-Vmeasured;
 error= desired- Vm;
 error=(error-10)*(0xc00-0x800)/-5;
 outport(base+16, error);
 }while(!kbhit());
}
```

Appendix D

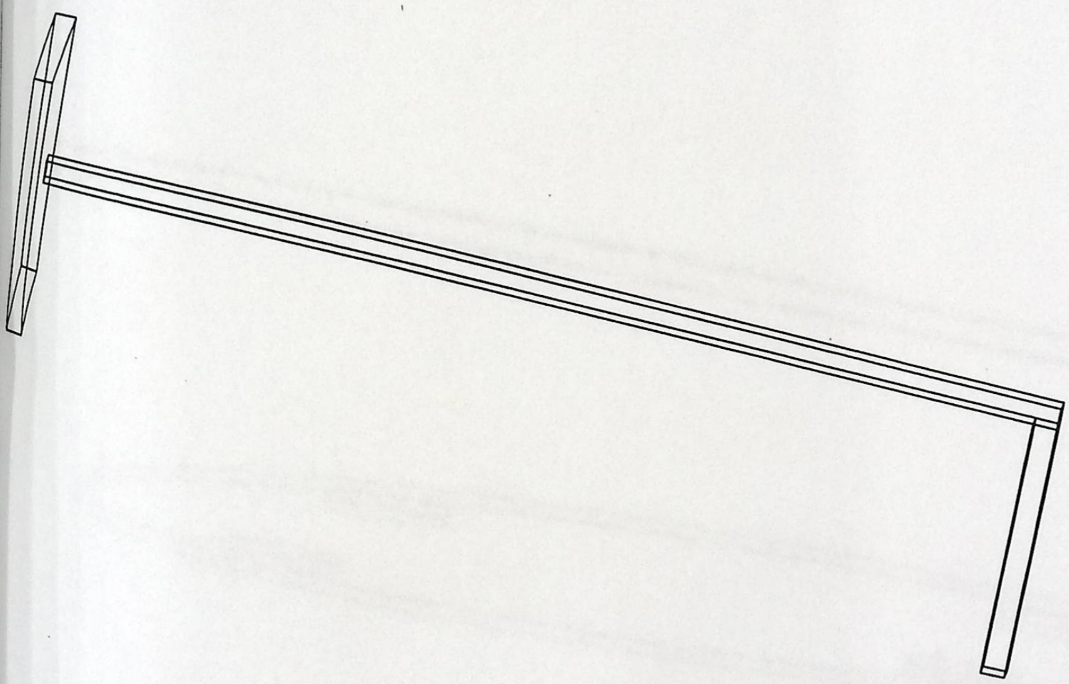

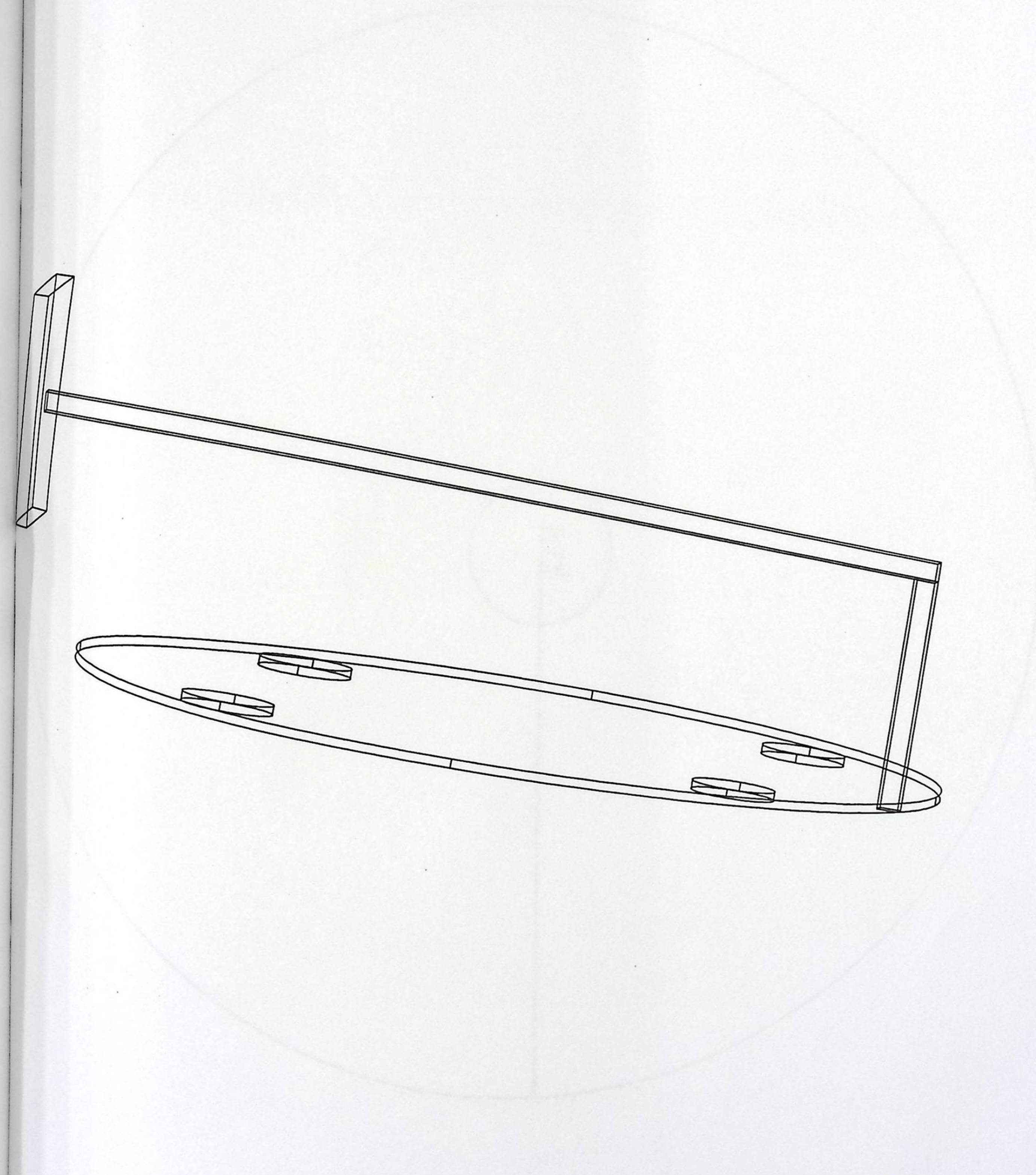

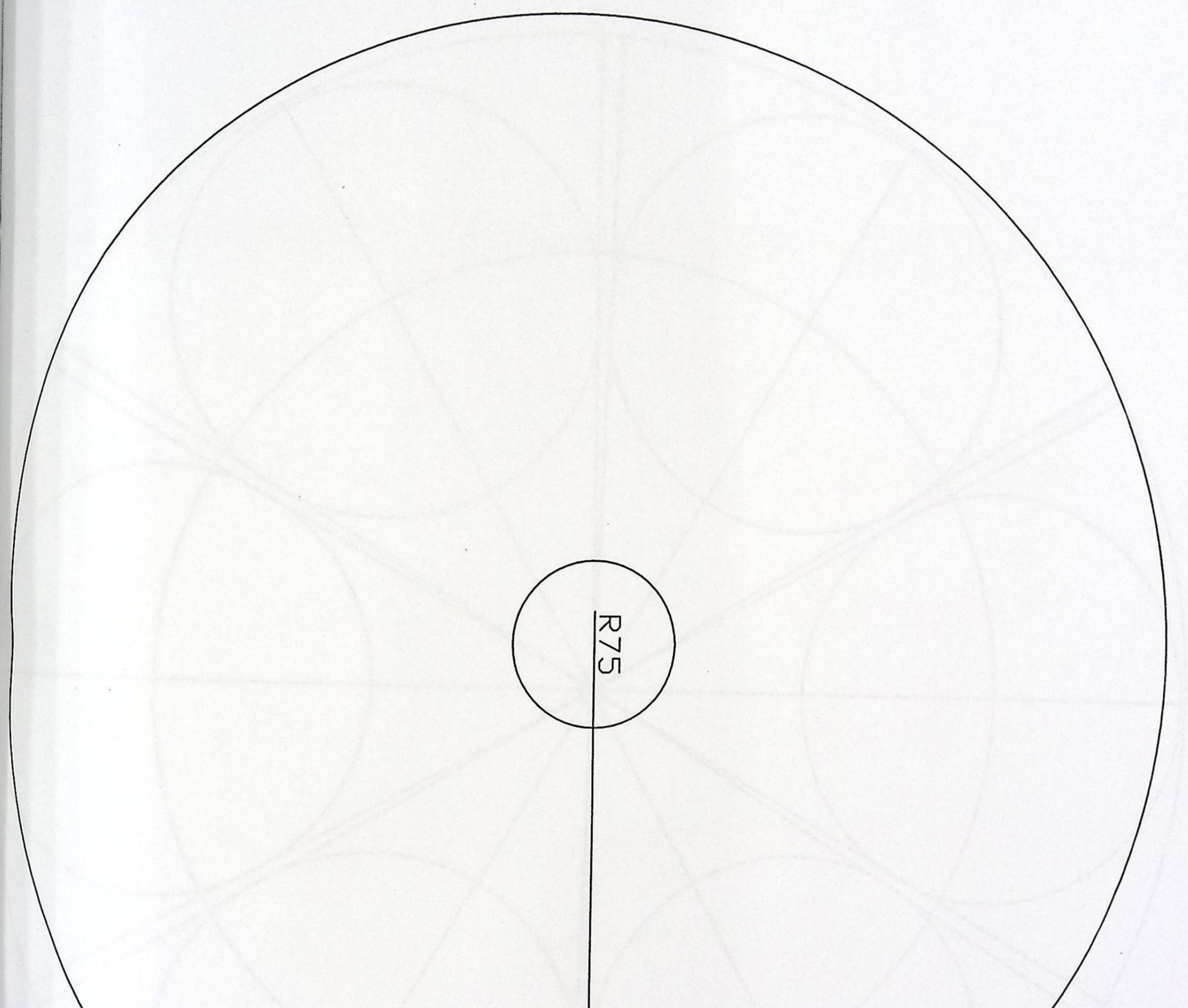
R75

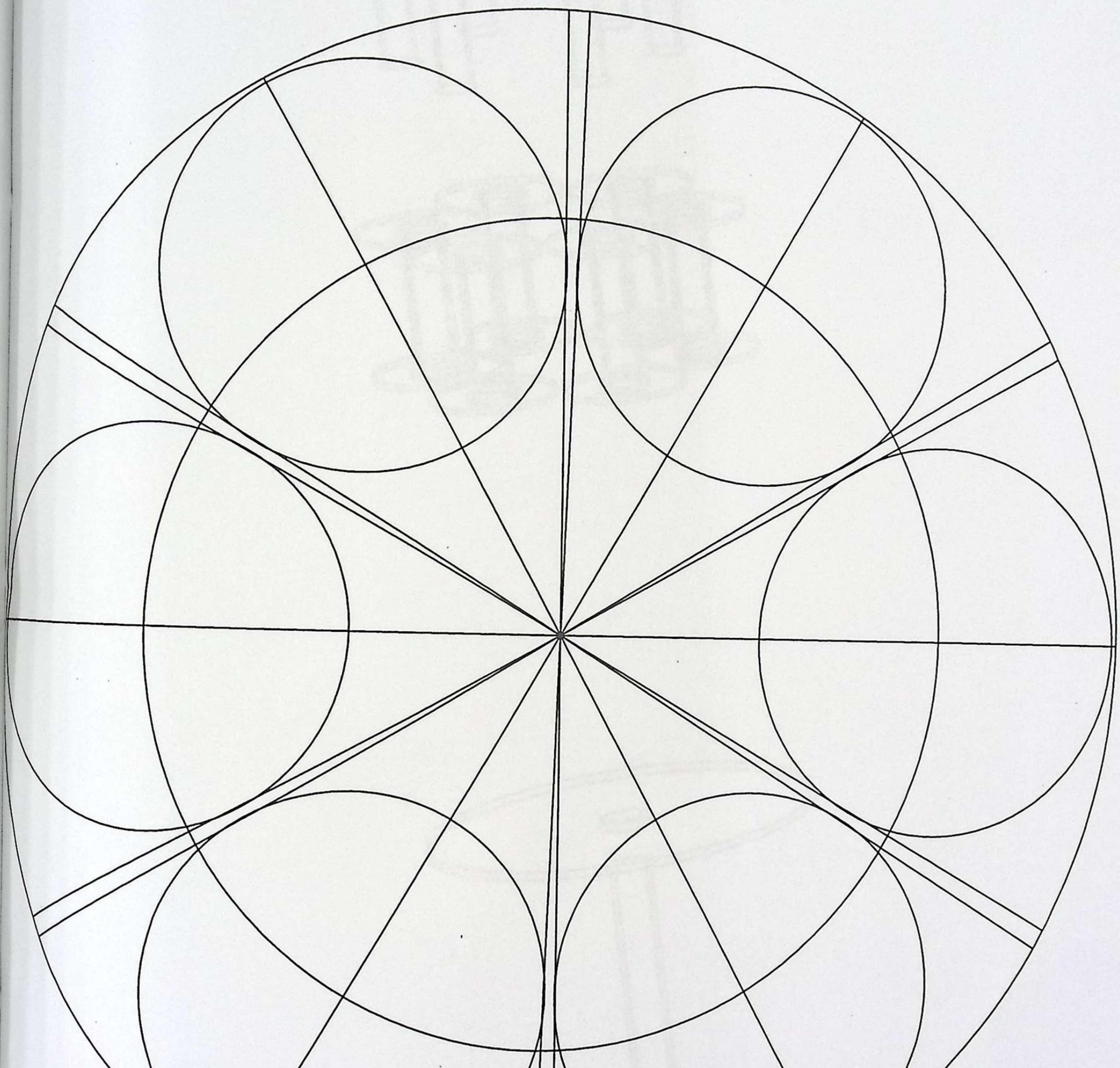

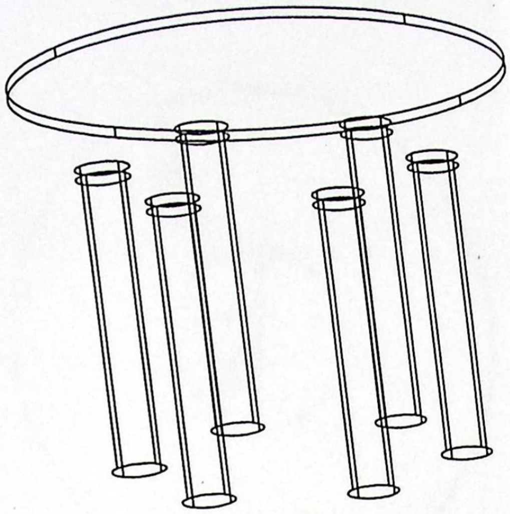

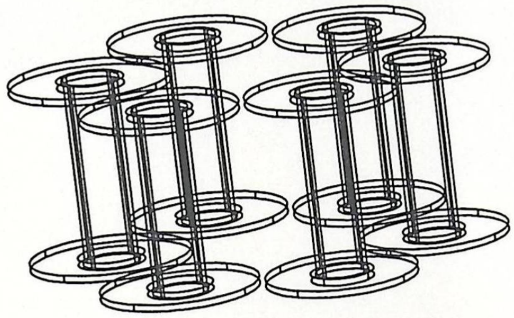

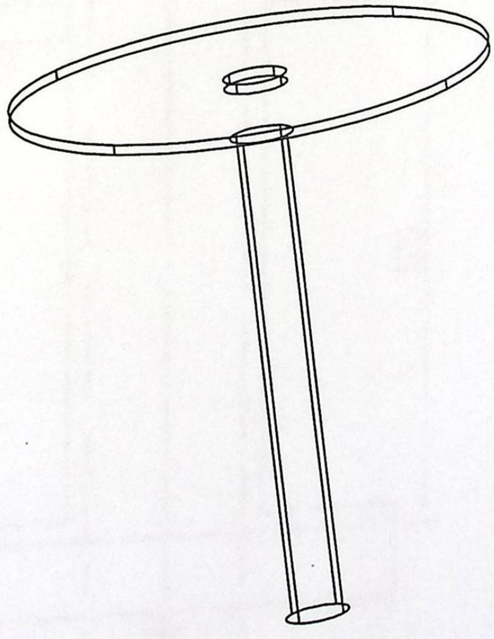

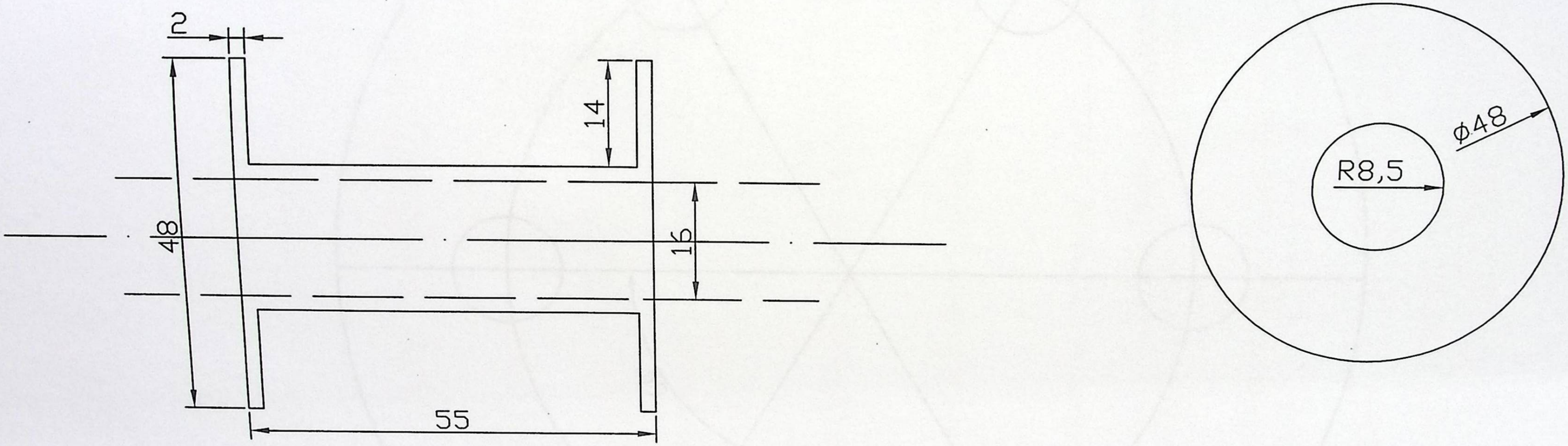
2
14
48
16
55
R8,5
ϕ48

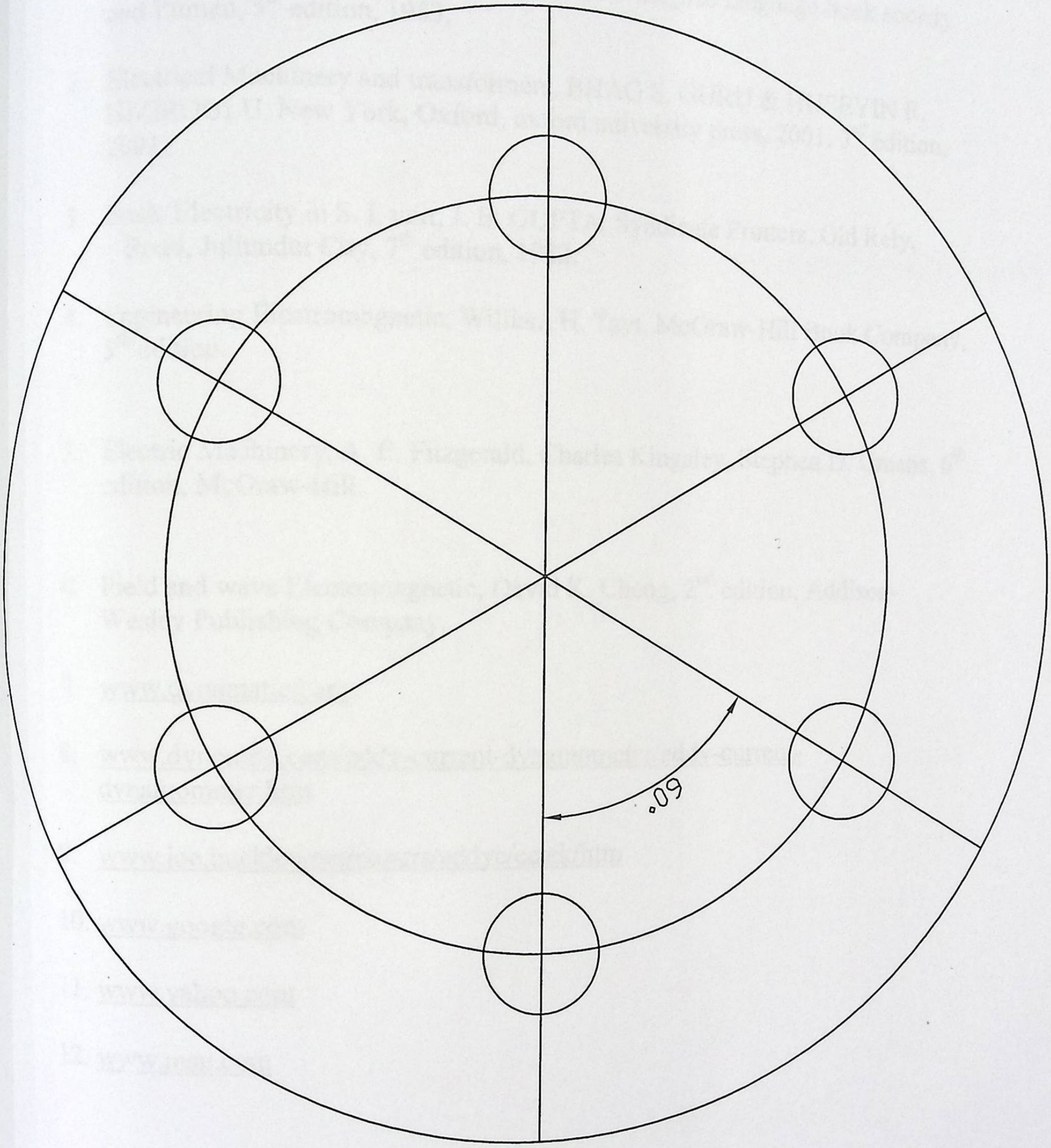
60°

References

1. alternating current machines, M. G. SAY, the English language book society and Pitman, 5th edition, 1983,

2. Electrical Machinery and transformers, BHAG S. GURU & HUSEYIN R. HIZIROGLU, New York, Oxford, oxford university press, 2001. 3rd edition, 2001.

3. Basic Electricity in S. I. unit, J. B. GUPTA, Syndicate Printers, Old Rely, Road, Jullundur City, 7th edition, 1982.

4. Engineering Electromagnetic, William H. Tayt, McGraw-Hill Book Company, 5th edition.

5. Electric Machinery, A. E. Fitzgerald, Charles Kingsley, Stephen D. Umans, 6th edition, McGraw-Hill.

6. Field and wave Electromagnetic, David K. Cheng, 2nd edition, Addison-Wesley Publishing Company.

7. www.dynamatic.com

8. www.dynomite.com/eddy-current-dynamometer/eddy-current-dynamometer.htm

9. www.joe.buckley.net/papers/eddyc/ectek/htm

10. www.google.com

11. www.yahoo.com

12. www.msn.com